From disturbances to nonlinear fitness and back

Shripad Tuljapurkar[1], Harman Jaggi[1], Samuel J. L. Gascoigne[2], Wenyun Zuo[1], Maja Kajin[2,3], and Roberto Salguero-Gómez[2]

[1]Stanford University, Department of Biology, CA, 94305, USA

[2]University of Oxford, Department of Biology, South Parks Road, Oxford OX1 3RB, UK

[3]University of Ljubljana, Department of Biology, Večna pot 111, 1000 Ljubljana, Slovenia

October 25, 2023

Abstract

A fundamental goal of Ecology is to predict how natural populations respond to disturbances. Accordingly, the last decades have witnessed key theoretical developments in stochastic demography and transient dynamics. However, both areas, have to date been largely disconnected. Here, we introduce an expression for the second derivatives of population growth rate with respect to demographic rates (*e.g.* survival-dependent state transitions and reproduction) with direct links to transient dynamics. We use this connection to develop a new mathematical framework showing how transient responses to pulse disturbances lead to a quantitative description of press disturbances. Second-derivatives of population growth rate with respect to said demographic rates are valuable as they quantify the degree of nonlinear selection acting on demographic rates and how environments shape the long-term performance of populations. Whilst valuable, previous methods to quantify second-order derivatives have heavily relied on vector calculus- potentially obscuring important demographic processes connected to second-order derivatives. Here we offer an intuitive method using perturbation theory and our approach is valid for any discrete-time, st(age)-based structured population model. Importantly, our new method implicates an intimate relationship between the nonlinear selection pressures acting on demographic rates with the emergent transient dynamics of populations over time. We showcase these relationships through mathematical proofs, connecting to Cohen's cumulative distance, and identifying a strong relationship between generation time across 439 unique plant and animal species (2690 population models). As such, this new method represents a valuable tool for population ecologists, comparative demographers, and conservation biologists to understand and protect structured populations in a changing world.

Introduction

The transient dynamics of structured systems (*e.g.*, populations, communities) are the system's responses following a pulse disturbance (Yang et al. 2008; Jentsch and White 2019). A pulse disturbance (such as an acute epidemic, fast invasion, or extreme, short weather event like a fire or hurricane) may perturb the system away from its stable state if it fails to resist the disturbance. As such transients are the dynamics that occur as the system returns back to the previous -or new- stable state (White et al. 2013; Tao et al. 2021). In contrast a press disturbance is a persistent change (e.g. global warming, river pollution) that alters the stable state itself in a more gradual manner (Donohue et al. 2016; Inamine et al. 2022). Though much attention has been paid both theoretically (Yang et al. 2008; Hastings 2001) and experimentally (Amor et al. 2020) to understand the responses of natural systems to pulse disturbances, not much theory or actual experimentation exists for their cousins: press disturbances (Inamine et al. 2022). Stage-structure population models represent a unique opportunity to marry both due to their temporal nature. These models treat time as a discrete entity, as the system is tracked every time unit, rather than continuously. As such, from the perspective of stage-structured models, a press disturbance can be viewed simply as a continuing series of pulses. Here, we focus on the consequences of that equivalence for natural populations by developing and applying new theory that explicitly links transient and stochastic population dynamics.

Here, we focus on populations structured by discrete stages (*e.g.*, age, size) and examined on discrete time: matrix population models (MPMs; (Caswell 2001b)). Under stationarity conditions, the population whose dynamics is described by a given MPM is at equilibrium, whereby the distribution of individuals in each of the states is defined by the stable structure distribution (hereafter SSD), a vector $\mathbf{u}_0$ and whose dynamics are guided by an exponential, fixed rate of growth, the population growth rate λ_0. A pulse disturbance that results in the deviation of the population vector from the SSD (*e.g.*, trophy hunting targets preferentially large/adult individuals (Traill et al. 2014), drought affects primarily juveniles in plant populations (Refsland and Fraterrigo 2018) will result in a transient dynamic as the population structure returns to the original -or a new (Capdevila et al. 2020)- SSD, as shown in the left panel of Fig 1. The pulse (*i.e.*, one-time) disturbance produces a change in population structure, and that change decays over time as the population structure returns to the SSD (indicated in the figure by vector $\mathbf{u}_0$).

In contrast, the effect of a press (*i.e.*, continued) disturbance can be thought of as the accumulation of the effect of repeated pulse disturbances, past and present, in a discrete time modelling framework. As illustrated in the right panel of Fig 1, the population structure reflects the current pulse disturbance, plus the decaying remnants of previous pulse disturbances. The cumulative result is to push population structure away from the original SSD to a new SSD (indicated in the figure by vector $\mathbf{u}_0'$).

We use this connection to develop a new mathematical framework showing how transient responses to pulse disturbances lead to a quantitative description of press disturbances. Press disturbances result in a linear change in the SSD but a nonlinear change in the population growth rate. Our

analysis focuses on small disturbances and yields new expressions for the first derivatives of the SSD and the second derivatives of population growth rate with respect to demographic rates.

Some general insights into the nonlinearity of fitness have come from Cohen's seminal work on matrices and matrix products (Cohen 1981; Cohen 1979a; Cohen 1979b; Cohen 1980) and have been used for instance by Drake (2005). Other insights are due to Caswell, who has long argued for the importance of second derivatives and developed methods for their computation (Caswell 1996, 2001b; Shyu and Caswell 2014), with more recent work by (McCarthy et al. 2008; Stott 2016). The most powerful computational method to date (Shyu and Caswell 2014) uses matrix-vector calculus and does not require non-dominant eigenvalues and eigenvectors, which are difficult to compute stably in general (Demmel 1986). Our approach is different from earlier work, both conceptually and mathematically.

In the next section, we describe the (known) effects of pulse disturbances in terms of transient dynamics. We use these results to show how the effect of a press disturbance on the SSD is obtained by analyzing a continued series of pulses in a discrete-time modelling framework. The same approach yields the effect of a press disturbance on the stable reproductive value. We illustrate these changes for an a stage-structured matrix population model for *Phaseolus lunatus* (commonly, Lima bean) from the COMADRE database (Salguero-Gómez et al. 2015). In the subsequent section, we turn to fitness as the long-run growth rate. There, we describe how the linear effect of a press disturbance on growth rate, the well known sensitivity (*i.e.*, first derivative), can be quantified. We use that simple approach to derive new expressions for the second derivatives of population growth rate. We illustrate these developments using MPM for *Phaseolus lunatus*. Then, we explain three useful aspects of the unexpected connection between the structure of transients and the nonlinearity of population-level fitness, thereby connecting our results to previous work by Cohen (1977) and more recently byJiang et al. (2022).

We close with a discussion of the multiple implications of our analyses: the novelty of the intimate connection we reveal between nonlinearity of the population growth rate with the transient dynamic response to a pulse; the fundamental role of local convexity/concavity in thinking about constraints in life histories, and about stabilizing/disruptive selection; the relationship between these results and the norm of response of life history strategies to fluctuating environments and disturbance regimes; the relevance of our current approach and results to the analysis of stochastic matrix population models; the relationship between what we do here and second-order perturbation theory (Stott 2016); the many implications of the linkage between our conceptual approach and linear response theory. And finally, the uses of our approach in studying the effect of disturbances in other ecological settings.

Pulse Disturbances and Transients

MPMs

We use matrix population models (MPMs) for structured populations in discrete time and in a constant environment. In this setting, the population is represented by a vector $\mathbf{n}(t)$ at time t, and a population projection matrix $\mathbf{B}$. The elements (b_{ij}) of said matrix represent the per-capita contributions of individuals in state j at t_0 to the realization of individuals in state i at t_1. These elements may incorporate one or more vital rates (*e.g.*, fertility is often the product of survival and fecundity), are ≥ 0 and so matrix $\mathbf{B}$ is non-negative; we assume that $\mathbf{B}$ is primitive (and so irreducible; *i.e.*, the life cycle graph defined by $\mathbf{B}$ contains the necessary information to describe pathways from all stages to all other stages). Then, this matrix has a dominant eigenvalue λ_0 with its corresponding right and left eigenvectors $\mathbf{u}_0, \mathbf{v}_0$ (Caswell 2001b). We normalize both vectors (*i.e.*, multiply by a suitable constant) so that the scalar product is $(\mathbf{v}_0, \mathbf{u}_0) = \mathbf{v}_0^T\, \mathbf{u}_0 = 1$. The superscript T indicates a transpose.

The stable stage distribution (SSD) is the vector $\mathbf{u}_0$, and the stable reproductive value vector is $\mathbf{v}_0$. We put these vectors together in a matrix

$$\mathbf{Q}_0 = \mathbf{u}_0\, \mathbf{v}_0^T, \tag{1}$$

Then the original population matrix can be written as a sum

$$\mathbf{B} = \lambda_0\, (\mathbf{Q}_0 + \mathbf{Q}_1), \tag{2}$$

$$\text{where } \mathbf{Q}_1 = \frac{1}{\lambda_0}\, (\mathbf{B} - \lambda_0\, \mathbf{Q}_0) \text{ is just the difference.} \tag{3}$$

Starting with an initial population vector $\mathbf{n}(0)$ and following the population over time using the MPM yields the customary result (see Appendix 1 for details) that

$$\frac{\mathbf{n}(t)}{\lambda_0^t} = \frac{\mathbf{B}^t}{\lambda_0^t}\mathbf{n}(0) = \left(\mathbf{Q}_0 + \mathbf{Q}_1^t\right)\, \mathbf{n}(0) \to \mathbf{Q}_0\, \mathbf{n}(0) = \left(\mathbf{v}_0^T\, \mathbf{n}(0)\right)\, \mathbf{u}_0, \tag{4}$$

so the population structure converges to the SSD and the growth rate does so to λ_0.

Effects of a Single Pulse Disturbance

The result of a pulse disturbance acting on a stable population is to change the population structure from the SSD to a sum of the SSD plus an added vector $\mathbf{u}_\perp$ that is perpendicular to the SSD. That additional 'perpendicularity' is precisely what sets the population away from its stationary equilibrium. Thus, after a pulse disturbance, the population vector is proportional to

$$\mathbf{u}_0 + \mathbf{u}_\perp.$$

Over the next time interval, if we assume constant environments and lack of density dependence, the demographic processes defined by the original matrix $\mathbf{B}$ act on the population again (otherwise $\mathbf{B}$ will change, and with it a new SSD will emerge). The part of the population structure that is the SSD will not change, so only the second term above will differ. This $\mathbf{u}_\perp$ is not affected by $\mathbf{Q}_0$ (as may be seen from equation (3), also the Appendix A.1). The net result is that, under these conditions, the new population structure will be proportional to

$$\mathbf{u}_0 + \mathbf{Q}_1\,\mathbf{u}_\perp.$$

This change is illustrated by the left panel in Fig 2. As time proceeds, the perpendicular component of the SSD ($\mathbf{u}_0$) shrinks and the population eventually returns to the SSD $\mathbf{u}_0$ (as shown in figure 2). The changes in the population structure are simply the transients,

$$\mathbf{u}_\perp, \mathbf{Q}_1\,\mathbf{u}_\perp, \mathbf{Q}_1^2\,\mathbf{u}_\perp, \mathbf{Q}_1^3\,\mathbf{u}_\perp, \ldots$$

and these eventually disappear as the population returns to the SSD. The convergence is illustrated by the bottom picture C in the left panel of Fig 2.

Press Disturbance as the Accumulation of Pulse Disturbances

Now let us turn to a press disturbance, in which the population matrix $\mathbf{B}$ is perturbed for all time, meaning that one or more demographic processes is permanently changed, so the MPM matrix $\mathbf{B}$ is changed to $\mathbf{B} + \mathbf{D}$ where the change is $\mathbf{D}$. For instance, if only one demographic process, say b_{23}, changes, then d_{23} is the only nonzero element of matrix $\mathbf{D}$. We visualize a one-off perturbation differently, as the same pulse disturbance at every time.

The right panel of Fig 2 shows how the effect of this press disturbance can alternatively be seen as the effect of a continued series of pulses of the same intensity and effect. The immediate result of a small pulse at time t_0 is that the population structure changes from the original SSD $\mathbf{u}_0$ (at time t_0) to the sum $\mathbf{u}_0 + \mathbf{z}^*$ in the next time step t_1, where (as detailed in the Appendix) the change is

$$\mathbf{z}^* = (\mathbf{I} - \mathbf{Q}_0)\,\frac{\mathbf{D}}{\lambda_0}\,\mathbf{u}_0. \tag{5}$$

Note that $\mathbf{z}^*$ is perpendicular to the SSD. If the perturbed structure was parallel to the SSD, then the new structure would be a multiple of the SSD, and by definition -when normalised to add up to 1- would result in the very SSD vector. Over the subsequent time interval, from time t_1 to time t_2, this initial change is acted on by the population matrix and becomes

$$\mathbf{Q}_1\,1z^*. \tag{6}$$

However, at t_2 there is also a new pulse, which produces a new change of size $\mathbf{z}^*$. Noe that at t_1 there

is also a new pulse, which produces a new change of size $\mathbf{z}^*$ at t_2. So, as shown in the right panel of Fig 2, at time 2 the new population structure is the sum

$$\mathbf{u}_0 + \mathbf{z}^* + \mathbf{Q}_1\,\mathbf{z}^*.$$

Continuing in this way (as in Fig 2), the effect of a press disturbance is the continued sum of its effects through discrete time

$$\mathbf{z}^* + \mathbf{Q}_1\,\mathbf{z}^* + \mathbf{Q}_1^2\,\mathbf{z}^* + \ldots.$$

This overall effect can be summed as a geometric series, so the new SSD is

$$\mathbf{u}_0' = \mathbf{u}_0 + (\mathbf{I} - \mathbf{Q}_1)^{-1}\,\mathbf{z}^*. \tag{7}$$

The process of convergence from the old to the new SSD is illustrated in the bottom right panel F of Fig 2).

Effects of a Press via a New Matrix

The preceding discussion about the effect of a press disturbance reveals the form of the resulting new SSD. Remember that the press changes the population matrix $\mathbf{B}$ to $\mathbf{B} + \mathbf{D}$, where the changes in all elements are small. We combine equation (5) and equation (7) in a particular way. First define the matrix

$$\mathbf{J}_0 = \frac{1}{\lambda_0}(\mathbf{I} - \mathbf{Q}_1)^{-1}\,(\mathbf{I} - \mathbf{Q}_0). \tag{8}$$

Then the new SSD produced by the press (as shown by (5 – 7)) is

$$\mathbf{u}_0 + \mathbf{Z},\ \text{where}\ \mathbf{Z} = \mathbf{J}_0\,\mathbf{D}\,\mathbf{u}_0. \tag{9}$$

As shown more formally in the Appendix 2, equation (9) is correct only to first order, meaning that the change we have obtained is the linear change (equivalently, the first derivative) of the SSD.

A precisely analogous argument can be made for the stable reproductive value. As a result of a small press disturbance, the stable reproductive value changes from $\mathbf{v}_0$ to

$$\mathbf{v}_0 + \mathbf{Y},\ \text{where}\ \mathbf{Y}^T = \mathbf{v}_0^T\,\mathbf{D}\,\mathbf{J}_0. \tag{10}$$

These changes in the SSD and stable reproductive value are key to the analyses below.

Example: Pulse and Press Disturbance for *Phaseolus lunatus* MPM

We use MPM for *Phaseolus lunatus* (COMPADRE database) to compare Pulse and Press disturbance as shown in Figure 3. For the pulse, we perturb Stage 1 of the SSD $\mathbf{u}_0$ and track the trajectory of the stage. As shown in top-left panel of Figure 3, after 10 time steps Stage 1 damps to the original

SSD $\mathbf{u}_0$ (dotted black line). Note that despite we only perturbed Stage 1, the transient effects can be observed in other stages as shown in the top-right panel of 3.

For the Press disturbance, we perturb elements (1,5) and (6,5) of the original MPM (increase by 80%). We again track the dynamics of Stage 1 of the original SSD ($\mathbf{u}_0$) and find Stage 1 converges to a new stable stage distribution, shown in dashed black line in the bottom-left panel of Figure 3.

Nonlinearity in Fitness

In our analyses of structured populations, the fitness of a life history is the long run growth rate λ_0 determined by the elements of matrix $\mathbf{B}$. To quantify the contributions of elements of $\mathbf{B}$ on λ_0, we can calculate the first-order impact (*i.e.*, sensitivities) of population growth rate as a function of these matrix elements ($\lambda_0(b_{pq})$). However, fitness can also vary as a function of pairs of matrix elements ($\lambda_0(b_{pq}, b_{kl})$, where $(p, q), (k, l)$ are row-column indices). Here, we explore nonlinearity in terms of the slope (first derivative) and curvature (second derivative) of these functions.

In this section, we show analyzing derivatives is the same thing as analyzing the effect of a press disturbance. For example, say we want to analyze the functional dependence of varying the matrix element b_{pq} on $\lambda_0(b_{pq})$. To do so, create a press disturbance that permanently changes only the pq element of the population projection matrix, with a new value say $(b_{pq} + d)$. In matrix terms, we change to a new population projection matrix $(\mathbf{B} + \mathbf{D})$ where only the (p, q) element of $\mathbf{D}$ is nonzero and equals d; all other elements of $\mathbf{D}$ equal zero. We provide an intuitive approach to evaluate the slope (first derivative) and the curvature (second derivative) of the function. Our work overcomes the limitation that responses of population dynamics to a change in vital rates are assumed linear (Hodgson and Townley 2004), but may not be as highlighted in Stott (2016).

Simple Approach to Slope *aka* Sensitivity

We begin with a simple method of finding the slope, the first derivative, of population growth rate with respect to pq, $\lambda_0(b_{pq})$, which is of course familiar as the sensitivity (Caswell 2001b),

$$s_{pq} = \frac{\partial \lambda_0}{\partial b_{pq}}. \tag{11}$$

We now describe a simple approach to compute the slopes. To explain, we start with a stationary stable population, in which the fraction of individuals in stage q is u_{0q}, the qth component of the SSD. In the next time interval, these individuals may transition to new states or stay in the same state (or die). To each final living state p, the initial fraction in state q contributes the amount $b_{pq}\, u_{0q}$. We weight this contribution by the final state's reproductive value v_{0p}, and identify $(v_{0p}\, b_{pq}\, u_{0q})$ as the weighted contribution of the $p \leftarrow q$ transition. The sum of these contributions over all initial and final states is λ_0 (as it should).

To apply the approach (discussed above) to a single element in the transition matrix, suppose that

we change the transition rate for the $p \leftarrow q$ transition from (b_{pq}) to $(b_{pq} + d)$, by adding some small d. Then (following the logic of the previous paragraph) the change in stable growth rate is the product of three terms:

a) the additional per-capita rate for that transition, *i.e.*, d;

b) the fraction of population that is subject to this change, *i.e.*, u_{0q};

c) the relative weight of ending in the final state q, *i.e.*, v_{0p}.

The product is: $d\, v_{0p}\, u_{0q}$. Dividing this change by d, we conclude that the first derivative of population growth rate to a disturbance of the $p \leftarrow q$ transition is

$$\frac{\partial \lambda_0}{\partial b_{pq}} = v_{0p}\, u_{0q} = s_{pq}. \tag{12}$$

So our simple method indeed yields the standard result (Caswell 2001b).

Using the new approach: Second derivatives

Just as press disturbances can impart small changes on individual, press disturbances can also shift co-varying vital rates (*e.g.*, early-life vs. late-life reproduction). Interestingly, the disturbance of two vital rates can also be used to quantify the second derivatives of population growth rate. For ease of exposition, say we create a press disturbance and change the pq and kl matrix elements to $b_{pq} + d$ and $b_{kl} + f$. We assume that d, f are small but we want to consider nonlinear changes, so we also include terms in $d^2, f\, d, f^2$.

Fig 4 illustrates two distinct ways of carrying out the above press disturbance, which must lead to the same overall change in fitness.

Say we use the first route, A to B and then B to D. In the change from A to B, our simple argument above shows that the change in fitness is the product

$$f\, v_0(k)\, u_0(l). \tag{13}$$

Now we want to make the change from B to D. But at B, equation (9) shows that (see Appendix for details) the SSD has already changed to $(\mathbf{u}_0 + f\, \mathbf{Z}_1)$ with

$$\mathbf{Z}_1 = u_{0l} \begin{pmatrix} J_{0,1k} \\ J_{0,2k} \\ \vdots \end{pmatrix}. \tag{14}$$

Also at B, equation (10) shows that the stable reproductive value has also already changed to $(\mathbf{v}_0 + f\, \mathbf{Y}_1)$ with

$$\mathbf{Y}_1^T = v_{0k} \begin{pmatrix} J_{0,l1} & J_{0,l2} & \dots \end{pmatrix}. \tag{15}$$

Now we are ready to use our approach to say that in the transition B to D, the fitness changes by the product of

a) the stable proportion in stage q, which equation (14) shows is $(u_{0q} + fZ_1(q))$,

b) the change in the rate, d,

c) the stable reproductive value in stage p, which equation (15) shows is $(v_{0p} + fY_1(p))$.

The product of these terms (ignore terms higher than quadratic, see Figure 4 for more) has to be added to the change (equation (13)) to get the total change in growth rate A to B to D,

$$f\, v_0(k)\, u_0(l) + d\, v_0(p)\, u_0(q) + f\, d\, \left(u_{0q}\, Y_1(p) + v_{0,p} Z_1(q)\right). \tag{16}$$

Using (14 – 15) the total change is the sum

$$\begin{aligned} \text{Linear change} &= f\, v_0(k)\, u_0(l) + d\, v_0(p)\, u_0(q), \\ &+ \\ \text{Nonlinear change} &= f\, d\, \left(u_{0q}\, v_{0k}\, J_{0,lp} + u_{0,l}\, v_{0,p}\, J_{0,qk}\right). \end{aligned} \tag{17}$$

We conclude that the nonlinearity is revealed by making two press disturbances. As shown in Fig 4, we could alternatively go from A to C and then C to D. That process involves distinct changes to the SSD and reproductive value. But we get the same final result as in equation (17). We can think about these changes in terms of the second derivatives of fitness (as explained further in the Appendix) to find

$$\frac{\partial^2 \lambda_0}{\partial b_{pq} \partial b_{kl}} = \left[s_{pl}\, J_{0,qk} + s_{kq}\, J_{0,lp}\right], \tag{18}$$

where we have used the sensitivities (equation (11)). Note that our expression for the second derivative is symmetric with respect to an exchange of the elements b_{pq}, b_{kl} (as it should be).

The curvature of fitness as measured by the second derivatives in equation (18) depends on the matrix $\mathbf{J}_0$. Consequently any analysis of second derivatives will provide detailed information about $\mathbf{J}_0$. The next section describes the multiple connections between $\mathbf{J}_0$ and transient dynamics. A computationally useful version of (18) uses Kronecker products (see Appendix A.33). We provide a detailed example to calculate second-derivatives using our perturbation approach for *Phaseolus lunatus* in Appendix A.5 and Figure A.1. The matrix for second-derivatives is depicted in Figure A.2. We also compute the second derivatives to show that our method yields the same result as the one in Shyu and Caswell (2014) (see Appendix A.6).

Transients and Nonlinearity

The previous section identifies the central role of the matrix $\mathbf{J}_0$ in defining the nonlinear response to a pulse disturbance and thus the second derivatives of fitness. Repeating the definition from equation (8),

$$\mathbf{J}_0 = \frac{1}{\lambda_0}(\mathbf{I} - \mathbf{Q}_1)^{-1}\,(\mathbf{I} - \mathbf{Q}_0).$$

Since matrix $\mathbf{Q}_1$ shapes the transient dynamics after a pulse, those transient dynamics also shape $\mathbf{J}_0$. The connection revealed between transients and nonlinearity of the dominant eigenvalue is unexpected and intimate. In this section we further illuminate this connection by three new results connecting $\mathbf{J}_0$ to transients.

Matrix $\mathbf{J}_0$ and cumulative distance to stability

An important metric to assess the difference between an observed stage distribution and the stable SSD is the cumulative distance to stability (Cohen 1979a). Several studies (Williams et al. 2011; White et al. 2013) have employed this metric. Here we point out that the matrix $\mathbf{J}_0$ actually determines the cumulative distance to stability.

As we know, any non-stable initial population distribution at time $t = 0$ converges towards the SSD. Following Cohen (1979a), at each later time t, the "distance" from stability is measured by summing the elements of the difference vector $f(t) = \lambda_0^{-t}\,\mathbf{n}(t) - \mathbf{Q}_0\,\mathbf{n}(0)$. Convergence means that this distance is decreasing, so the cumulative vector $F(t) = \sum_{m=0}^{(t-1)} f(m)$ should have a limit. For an initial population vector $\mathbf{n}(0)$ Cohen showed this limit to be

$$\lim_{t\to\infty} F(t) = \left[\left(\mathbf{I} + \mathbf{Q}_0 - \frac{\mathbf{B}}{\lambda_0}\right)^{-1} - \mathbf{Q}_0\right]\mathbf{n}(0). \tag{19}$$

We find that Cohen's cumulative distance is just

$$\lim_{t\to\infty} F(t) = \mathbf{J}_0\,\mathbf{n}(0), \tag{20}$$

as shown in the Appendix. Thus $\mathbf{J}_0$ is directly related to the asymptotic cumulative distance to stability.

Structure of $\mathbf{J}_0$ for population matrices with distinct eigenvalues

When the matrix population model $\mathbf{B}$ has distinct eigenvalues (and linearly independent eigenvectors), we can write the spectral decomposition of $\mathbf{B}$ (Good 1969) as: $\mathbf{B} = \lambda_0\,\mathbf{u}_0\,\mathbf{v}_0^\dagger + \lambda_1\,\mathbf{u}_1\,\mathbf{v}_1^\dagger + \lambda_2\,\mathbf{u}_2\,\mathbf{v}_2^\dagger + \cdots = \sum_{j=0}\lambda_j\,e^{\mathbf{i}\omega_j}\,\mathbf{u}_j\,\mathbf{v}_j^\dagger$, where $\mathbf{u}_j$ and $\mathbf{v}_j$ are right and left eigenvectors of $\mathbf{B}$. In this case, we write the

higher eigenvalues (maybe complex) as $\lambda_j = e^{(r_j + \mathbf{i}\omega_j)}$ for $j \geq 1$ and write the eigenvalue ratio as:

$$\frac{\lambda_j}{\lambda_0} = \frac{e^{(r_j + \mathbf{i}\omega_j)}}{e^{r_0}} = \tau_j \, e^{\mathbf{i}\omega_j}$$

where $\tau_j = e^{r_j - r_0}$ and $\tau_j < 1$; the τ_j are the inverse damping ratios Caswell (2001a). The spectral decomposition for $\mathbf{B}$, and the definition equation (1) show that

$$\mathbf{Q}_1 = \sum_{j \geq 1} \tau_j \, e^{\mathbf{i}\omega_j} \, \mathbf{u}_j \, \mathbf{v}_j^{\dagger}. \tag{21}$$

We can now write an explicit expression for $\mathbf{J}_0$ (details in Appendix) as

$$\mathbf{J}_0 = \sum_{j \geq 1} \frac{\mathbf{u}_j \, \mathbf{v}_j^{\dagger}}{(1 - \tau_j \, e^{\mathbf{i}\omega_j})}. \tag{22}$$

This is a spectral decomposition of $\mathbf{J}_0$ (excluding the eigenvector $\mathbf{u}_0$ for which the eigenvalue is 0). Thus the vectors $\mathbf{u}_j$, $\mathbf{v}_j$ are right, left eigenvectors of $\mathbf{J}_0$ corresponding to eigenvalue $\left(1 - \tau_j \, e^{\mathbf{i}\omega_j}\right)^{-1}$. One consequence is that the dominant eigenvalue of $\mathbf{J}_0$ depends on the damping ratio τ_1.

Matrix $\mathbf{J}_0$ and Asymptotics of Transients

The preceding discussion implies that the dominant eigenvalue of $\mathbf{J}_0$ is a quantitative measure of the asymptotic convergence of transients. Previous studies have shown that life history significantly influences transient dynamics of a population (Haridas and Tuljapurkar 2007).

Jiang et al. (2022) found a strong correlation between transients (using damping time) with generation time (T_c), a key life history trait (Gaillard et al. 2005). This finding led us to hypothesize that the dominant eigenvalue of $\mathbf{J}_0$ is also correlated with life history traits. To examine this hypothesis, we analyzed 439 unique age and stage- structured species (after correcting for phylogenetic inertia) using the COMADRE Animal Matrix Database (Salguero-Gómez et al. 2016), the COMPADRE Plant Matrix Database (Salguero-Gómez et al. 2015), and previously published mammalian database in Jiang et al. (2022). As shown in Figure 5, we find that the dominant eigenvalue of $\mathbf{J}_0$ is indeed strongly correlated with generation time T_c on the log-log scale (Figure 5).

Thus the higher (subdominant) eigenvalues and eigenvectors of $\mathbf{B}$ completely determine our matrices $\mathbf{Q}_1$ and $\mathbf{J}_0$. Of course, the relationships in this subsection are of little computational use if there are repeated eigenvalues, or if we cannot compute the eigenvalues accurately. But even then, the powers of $\mathbf{Q}_1$ and thus the matrix $\mathbf{J}_0$ describe the transient dynamics of the population matrix. This connection is described by Cohen (1979a) using a cumulative distance measure, and we now show that is directly given by our matrix $\mathbf{J}_0$.

Discussion

Population ecology has, over recent decades, acquired a sizeable arsenal of tools to approximate and quantify how natural populations respond to environmental stochasticity (Roughgarden 1975; Doak et al. 1994; Medeiros et al. 2023). In parallel, the field has also made important progress in the understanding of how natural populations respond to one-off (*i.e.*, pulse) disturbances (Jentsch and White 2019). However, natural populations are rarely exposed to a single disturbance that fades fast enough (or where there is enough time) for the population to go back to stationary equilibrium. Here, we propose a novel approach to examine how natural populations respond to press disturbances. This approach is based on known results about pulse disturbances and transients to analyze press disturbances and nonlinear responses of population growth rate to demographic rate perturbations. Our results reveal an intimate -and unexpected- connection between the nonlinearity of population growth rate to vital rates, and transient dynamics. These findings provide valuable insights into the ways populations respond to disturbance regimes, with multiple implications for ecological modelling, ecological forecasting, and comparative demography.

A key contribution of this study is the introduction of a new approach for calculating the second derivatives of long-term population growth rates with respect to their underlying vital rates in st(age)-structured populations (*e.g* matrix population models, Caswell (2001b) and Ellner et al. (2016)). This approach, which is both intuitive and powerful, enables researchers to explore the impact of linear and nonlinear selection on vital rates such as survival, growth, and reproduction. Our approach unlocks a deeper understanding of the factors influencing population dynamics. Indeed, the second derivative of population growth rate with respect to all vital rates that constitute an MPM provides information of important evolutionary implications (Doak et al. 1994; Brodie et al. 1995; Vasseur and Fox 2007; Shyu and Caswell 2014). Namely, these second derivatives inform on: (1) whether a function (in our case, the average fitness of individuals in the population) changes linearly as vital rates are perturbed (*e.g.*, Caswell (2001b)); 2) if nonlinear, whether fitness follows a concave (negative self-second derivative) or convex (positive self-second derivative) function for a specific vital rate (*e.g.*, Caswell (2001b)); and (3) if the second derivative of fitness with respect to vital rates is positive for observed life histories, then the examined value corresponds to a local minimum, and *vice versa* if the second derivative of fitness is negative at a critical point, then that critical point corresponds to a local maximum (Brodie et al. 1995). Here, statement (3) is of particular evolutionary and ecological importance, because it provides valuable insights into the stability of populations. Indeed, this way of thinking about the dynamics of a population in a stochastic environment enables us to conclude - based on a given second derivative value - whether fitness will increase as vital rates are perturbed or not. In other words, if a local maximum is evidenced, then further disturbances of a given (or all) vital rate(s) will inevitably only lead to the decrease in fitness. This information is particularly valuable when examining population forecasts of species to climate extremes (Thibault and Brown 2008), and selection for optimal life history strategies for a given environment (Tuljapurkar et al. 2009). As such, we argue that our second

derivative approach is particularly valuable for active research in human demography (*e.g.*, McLeod and Day (2019)), population ecology (*e.g.*, Feng et al. (2022)), and comparative biology (*e.g.*, Compagnoni et al. (2021)). We emphasize the applicability of second-order perturbation theory, such as Kato's theory (Kato 2013), in describing the nonlinear response in structured populations. This line of work opens up possibilities for using this method in multiple contexts, such as community composition and nonlinear multi-species interactions (Bender et al. 1984; Collins et al. 2020), broadening the scope of its application.

Our findings reveal a robust link between the matrix $\mathbf{J}_0$ and short-term population dynamics in the aftermath of a perturbation. When a pulse disturbance perturbs the vital rates of a st(age)-structured population, the resulting nonlinear response in fitness can be quantified through the second-order derivative of the population growth rate. Here, we have formally defined the second derivative of the population growth rate in terms of the matrix $\mathbf{J}_0$ (See appendix). This formalization establishes a clear association between the nonlinear response in fitness and transient dynamics. These transient dynamics, stemming from a pulse disturbance, are characterized by the matrix Q_1, which is a constituent element in the $\mathbf{J}_0$ equation (7), and consequently, it shapes $\mathbf{J}_0$. This interconnection gives rise to second-order fitness derivatives that exhibit nonlinear selection pressures, displaying concavity when the self-second derivative is negative and convexity when positive (Levine et al. 2022), with these effects being influenced by the transient phases in the population's dynamic trajectory.

In the realm of community ecology, it has been demonstrated that the interplay between pulse and press disturbances can lead to intricate, nonlinear interactions within ecological communities (Inamine et al. 2022). Pulse disturbances afford opportunities for select species during transient phases, while press disturbances can induce nonlinear, often unpredictable shifts in species performance over time. These interactions cascade through the community, affecting species composition and abundance in ways that defy straightforward predictions offered by linear population dynamics models. Our approaches, explicitly linking transient dynamics to well-established approaches to quantify stochastic demographics, coupled with the ability of st(age)-structured models to incorporate intra- and inter-specific effects (*e.g.*, Kayal et al. (2018) and Adler et al. (2012)) offer unique opportunities to integrate responses of natural systems across levels of biological organisation: from individuals, to populations, to full communities. This integration is a primary need in the field of ecological resilience (Capdevila et al. 2021).

Our findings also suggest a parallel in the context of population dynamics. The co-occurrence of press and pulse disturbances is a plausible scenario, particularly in light of increasing environmental stochasticity. Conceptually, the mechanics of press disturbances can be understood as an amalgamation of multiple, back-to-back pulse disturbances. Given that a single pulse disturbance, along with the ensuing transient behavior, indirectly impacts the nonlinearity of fitness responses, we posit that long-term press disturbances, along with the associated transients dislocating populations from their original stable state, will yield a more intricate and nonlinear response in fitness. In this study, we have elucidated the mathematical framework underpinning the connection between transients and

nonlinearity in fitness. This connection helps in understanding transient dynamics and resilience metrics in structured populations, offering new avenues for exploration in population ecology and comparative demography.

An important area for future investigation in this regard is the link between the environmental response of vital rates and the environmental response of fitness. Specifically, the examination of environment-vital rate reaction norms in natural populations holds potential for further research in understanding the causes of trait variance in populations over time and the plasticity of life history processes in response to environmental changes (Klingenberg 2019). Our results point to new directions to examine population responses in stochastic environments. To see why, note that way a population fares in a stochastic environment can be viewed in terms of a sequence of unequal pulses, and their cummulative effects (as shown in Figure 1). So for example, we can examine how shifts in mean, variance, and temporal autocorrelation may impact a population's ability to persist (Drake 2005; Vasseur and Fox 2007). We highlight the need for further research on the relationships between first-order and second-order derivatives of population growth rate with respect to vital rates as an yet unexplored area offering exciting opportunities for the field of ecological forecast, has hinted at by Shyu and Caswell (2014). In summary, the theoretical developments presented here, together with the findings that a tight connection exists between transient dynamics and stochastic dynamics open up new avenues in the study of structured demography. We argue that the potential implications are wide-ranging, and include the fields of formal demography, population ecology, and comparative demography. The insights into the connections between nonlinearity, transients, and selection pressures are expected to have a significant impact on future research in these areas, providing valuable tools for understanding and managing population dynamics in a changing world.

References

Adler, Peter B, Harmony J Dalgleish, and Stephen P Ellner (2012). "Forecasting plant community impacts of climate variability and change: when do competitive interactions matter?" *Journal of Ecology* 100.2, pp. 478–487.

Amor, DR, C Ratzke, and J Gore (2020). *Transient invaders can induce shifts between alternative stable states of microbial communities. Sci Adv 6: eaay8676.*

Bender, Edward A, Ted J Case, and Michael E Gilpin (1984). "Perturbation experiments in community ecology: theory and practice". *Ecology* 65.1, pp. 1–13.

Brodie, Edmund D, Allen J Moore, and Fredric J Janzen (1995). "Visualizing and quantifying natural selection". *Trends in Ecology & Evolution* 10.8, pp. 313–318.

Capdevila, Pol, Iain Stott, Maria Beger, and Roberto Salguero-Gómez (2020). "Towards a comparative framework of demographic resilience". *Trends in Ecology & Evolution* 35.9, pp. 776–786.

Capdevila, Pol et al. (2021). *Reconciling resilience across ecological systems, species and subdisciplines.*

Caswell, H. (2001a). *Matrix population models: construction, analysis and interpretation.* 2nd. Sunderland, Mass.: Sinauer associates, Sunderland, Mass.

Caswell, Hal (1996). "Second derivatives of population growth rate: calculation and applications". *Ecology*, pp. 870–879.

— (2001b). *Matrix Population Models: Construction, Analysis, and Interpretation.* 2nd. Sinauer Associates Inc., Sunderland, MA.

Cohen, J.E. (1977). "Ergodicity of age structure in populations with Markovian vital rates, III: finite-state moments and growth rate; an illustration". *Advances in Applied Probability*, pp. 462–475.

— (1979a). "The cumulative distance from an observed to a stable age structure". *SIAM Journal on Applied Mathematics* 36.1, pp. 169–175.

— (1980). "Convexity properties of products of random nonnegative matrices". *Proceedings of the National Academy of Sciences* 77.7, pp. 3749–3752.

Cohen, Joel E (1981). "Convexity of the dominant eigenvalue of an essentially nonnegative matrix". *Proceedings of the American Mathematical Society* 81.4, pp. 657–658.

— (1979b). "Random evolutions and the spectral radius of a non-negative matrix". *Mathematical Proceedings of the Cambridge Philosophical Society* 86.2, pp. 345–350. DOI: 10.1017/S0305004100056164.

Collins, Scott L et al. (2020). "Press–pulse interactions and long-term community dynamics in a Chihuahuan Desert grassland". *Journal of Vegetation Science* 31.5, pp. 722–732.

Compagnoni, Aldo et al. (2021). "Herbaceous perennial plants with short generation time have stronger responses to climate anomalies than those with longer generation time". *Nature Communications* 12.1, p. 1824.

Demmel, James Weldon (1986). "Computing stable eigendecompositions of matrices". *Linear Algebra and its Applications* 79, pp. 163–193.

Doak, Daniel, Peter Kareiva, and Brad Klepetka (1994). "Modeling population viability for the desert tortoise in the western Mojave Desert". *Ecological Applications* 4.3, pp. 446–460.

Donohue, Ian et al. (2016). "Navigating the complexity of ecological stability". *Ecology letters* 19.9, pp. 1172–1185.

Drake, J.M. (2005). "Population effects of increased climate variation". *Proceedings of The Royal Society B* 272.1574, p. 1823.

Ellner, Stephen P, Dylan Z Childs, Mark Rees, et al. (2016). "Data-driven modelling of structured populations". *A practical guide to the Integral Projection Model. Cham: Springer*.

Feng, Tao, Hongjuan Zhou, Zhipeng Qiu, and Yun Kang (2022). "Impacts of demographic and environmental stochasticity on population dynamics with cooperative effects". *Mathematical Biosciences* 353, p. 108910.

Gaillard, J.M. et al. (2005). "Generation Time: A Reliable Metric to Measure Life-History Variation among Mammalian Populations". *American Naturalist* 166.1, pp. 119–123.

Good, Irving John (1969). "Some applications of the singular decomposition of a matrix". *Technometrics* 11.4, pp. 823–831.

Haridas, CV and Shripad Tuljapurkar (2007). "Time, transients and elasticity". *Ecology Letters* 10.12, pp. 1143–1153.

Hastings, Alan (2001). "Transient dynamics and persistence of ecological systems". *Ecology Letters* 4.3, pp. 215–220.

Hodgson, David J and Stuart Townley (2004). "Methodological insight: linking management changes to population dynamic responses: the transfer function of a projection matrix perturbation". *Journal of Applied Ecology* 41.6, pp. 1155–1161.

Horvitz, Carol C and Douglas W Schemske (1995). "Spatiotemporal variation in demographic transitions of a tropical understory herb: projection matrix analysis". *Ecological monographs* 65.2, pp. 155–192.

Inamine, Hidetoshi et al. (2022). "Pulse and Press Disturbances Have Different Effects on Transient Community Dynamics". *The American Naturalist* 200.4, pp. 571–583.

Jentsch, Anke and Peter White (2019). "A theory of pulse dynamics and disturbance in ecology". *Ecology* 100.7, e02734.

Jiang, Sha et al. (2022). "Reproductive dispersion and damping time scale with life-history speed". *Ecology Letters* 25.9, pp. 1999–2008.

Karlin, S. and H.M. Taylor (1975). *A first course in stochastic processes*. Academic Press.

Kato, Tosio (1976). *Perturbation theory for linear operators*. Vol. 132. Springer Science & Business Media.

— (2013). *Perturbation theory for linear operators*. Vol. 132. Springer Science & Business Media.

Kayal, Mohsen et al. (2018). "Predicting coral community recovery using multi-species population dynamics models". *Ecology Letters* 21.12, pp. 1790–1799.

Klingenberg, Christian Peter (2019). "Phenotypic plasticity, developmental instability, and robustness: The concepts and how they are connected". *Frontiers in Ecology and Evolution* 7, p. 56.

Levine, Jacob I, Jonathan M Levine, Theo Gibbs, and Stephen W Pacala (2022). "Competition for water and species coexistence in phenologically structured annual plant communities". *Ecology letters* 25.5, pp. 1110–1125.

McCarthy, Dominic, Stuart Townley, and Dave Hodgson (2008). "On second order sensitivity for stage-based population projection matrix models". *Theoretical Population Biology* 74.1, pp. 68–73.

McLeod, David V and Troy Day (2019). "Social evolution under demographic stochasticity". *PLoS computational biology* 15.2, e1006739.

Medeiros, Lucas P et al. (2023). "Ranking species based on sensitivity to perturbations under non-equilibrium community dynamics". *Ecology Letters* 26.1, pp. 170–183.

Refsland, Tyler and Jennifer Fraterrigo (2018). "Fire increases drought vulnerability of Quercus alba juveniles by altering forest microclimate and nitrogen availability". *Functional Ecology* 32.10, pp. 2298–2309.

Roughgarden, Jonathan (1975). "A simple model for population dynamics in stochastic environments". *The American Naturalist* 109.970, pp. 713–736.

Salguero-Gómez, Roberto et al. (2015). "The compadre P lant M atrix D atabase: an open online repository for plant demography". *Journal of Ecology* 103.1, pp. 202–218.

Salguero-Gómez, Roberto et al. (2016). "COMADRE: a global data base of animal demography". *Journal of Animal Ecology* 85.2, pp. 371–384.

Shyu, Esther and Hal Caswell (2014). "Calculating second derivatives of population growth rates for ecology and evolution". *Methods in Ecology and Evolution* 5.5, pp. 473–482.

Stott, Iain (2016). "Perturbation analysis of transient population dynamics using matrix projection models". *Methods in Ecology and Evolution* 7.6, pp. 666–678.

Tao, Yun et al. (2021). "Transient disease dynamics across ecological scales". *Theoretical Ecology* 14.4, pp. 625–640.

Thibault, Katherine M and James H Brown (2008). "Impact of an extreme climatic event on community assembly". *Proceedings of the National Academy of Sciences* 105.9, pp. 3410–3415.

Traill, Lochran W, Susanne Schindler, and Tim Coulson (2014). "Demography, not inheritance, drives phenotypic change in hunted bighorn sheep". *Proceedings of the National Academy of Sciences* 111.36, pp. 13223–13228.

Tuljapurkar, Shripad, Jean-Michel Gaillard, and Tim Coulson (2009). "From stochastic environments to life histories and back". *Philosophical Transactions of the Royal Society B: Biological Sciences* 364.1523, pp. 1499–1509.

Vasseur, David A and Jeremy W Fox (2007). "Environmental fluctuations can stabilize food web dynamics by increasing synchrony". *Ecology Letters* 10.11, pp. 1066–1074.

White, J Wilson et al. (2013). "Transient responses of fished populations to marine reserve establishment". *Conservation Letters* 6.3, pp. 180–191.

503 Williams, Jennifer L et al. (2011). "Distance to stable stage distribution in plant populations and
504 implications for near-term population projections". *Journal of ecology* 99.5, pp. 1171–1178.
505 Yang, Louie H, Justin L Bastow, Kenneth O Spence, and Amber N Wright (2008). "What can we learn
506 from resource pulses". *Ecology* 89.3, pp. 621–634.

Figures

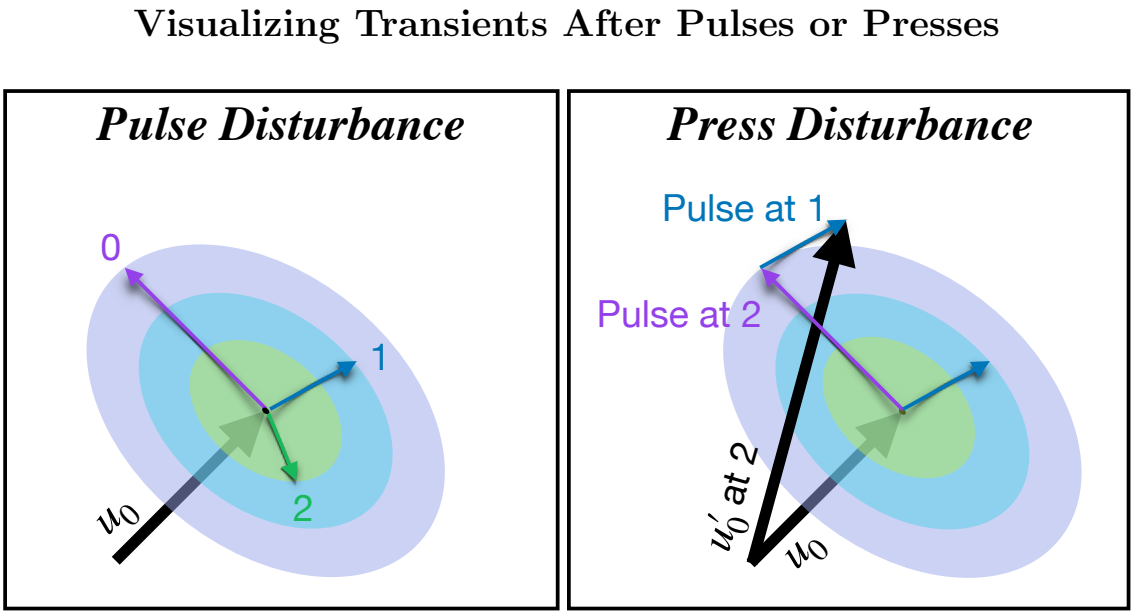

Figure 1: The left panel illustrates transient dynamics of a structured population after a pulse (one-time) disturbance. At time t_0, the purple arrow depicts pulse disturbance. After one time step, at time t_1, the pulse decays showing subsequent rotation and shrinkage of deviations from the SSD $\mathbf{u}_0$ (blue arrow), and then at time t_2 (green arrow), *etc.*. Note that eventually, the structure converges to original stable structure $\mathbf{u}_0$. In the right panel, results of a press (permanent) disturbance are illustrated as the sum of the effects of the current (at time t_2) pulse, and the decaying effects of past pulses (blue arrow at time t_1). In the case of press disturbance (to matrix elements), the convergence is to a new stable structure $\mathbf{u}_0'$ as shown in the right panel.

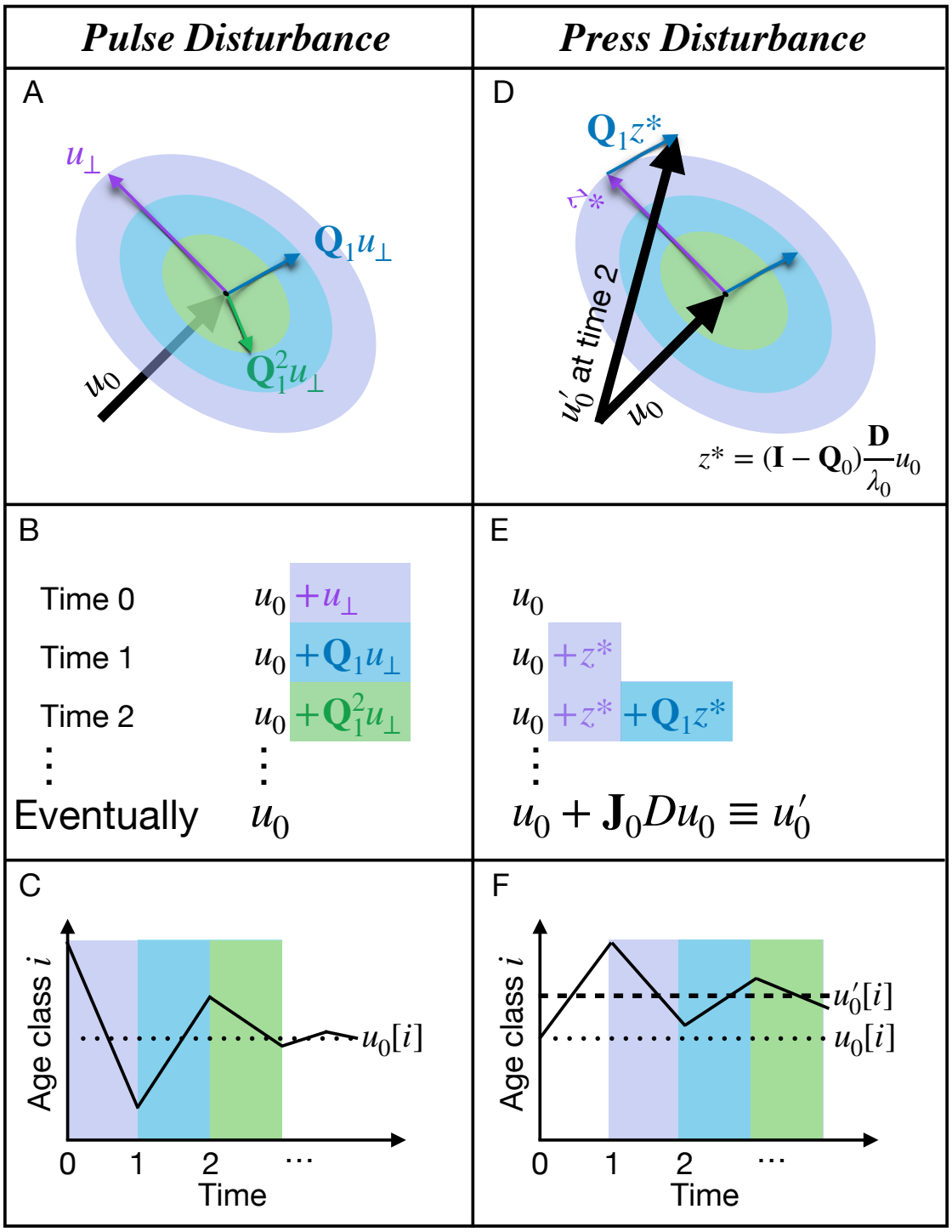

Figure 2: Left panel: A, transient dynamics after a pulse (one-time) pulse at t_0, showing subsequent (at t_1 and t_2) rotation and shrinkage of deviations from the SSD $\mathbf{u}_0$; B, explicit form of transient contribution to structure, with eventual return to SSD; C, decaying transients in one component of the population structure. Right panel: D, result of a press (permanent) disturbance, as a sum of the effect of the current (at t_2) pulse, and the decaying effects of past pulses at times t_1 and t_0 (only two are shown); E, explicit form of population structure, with eventual convergence to the new SSD; F, accumulation of changes in the SSD over time.

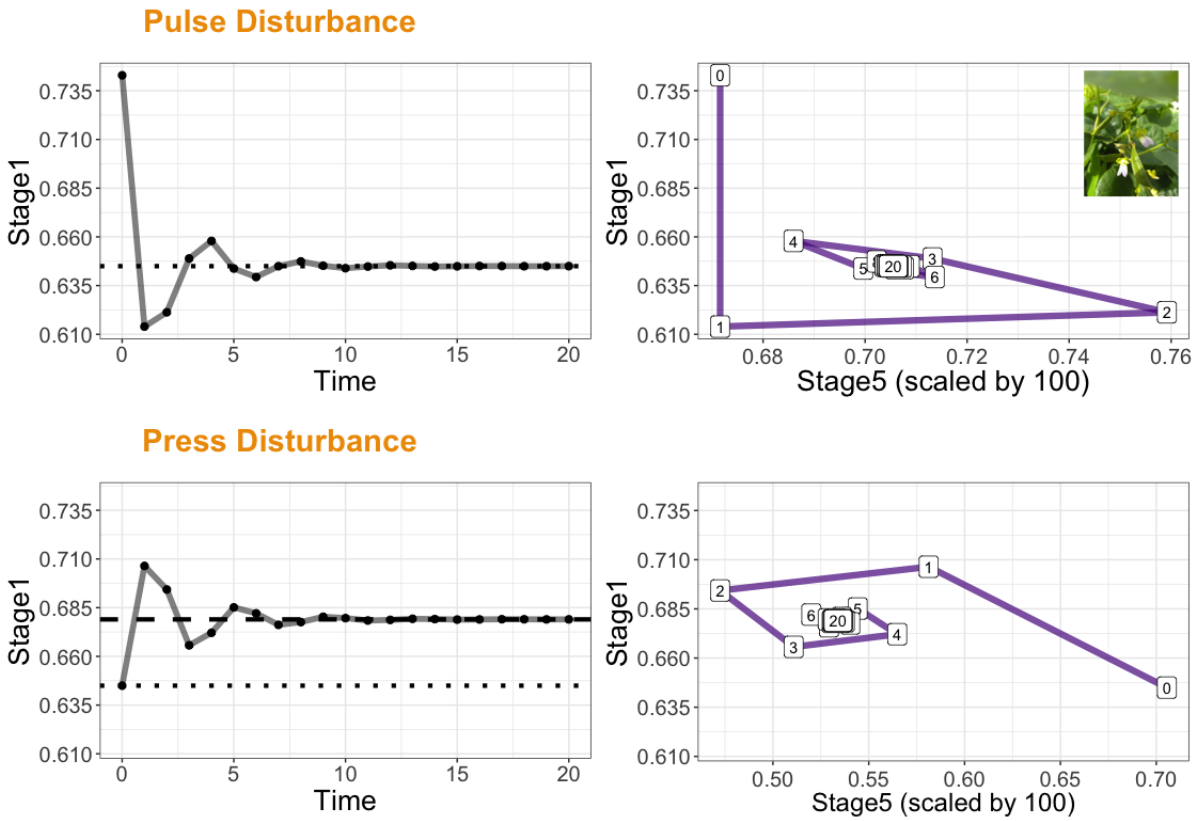

Figure 3: Pulse and Press disturbances for *Phaseolus lunatus*. The top two panels follow transient dynamics in Stage 1 after a pulse disturbance to the Stable Stage Distribution ($\mathbf{u}_0$) (Stage 1 perturbed). On the top-left panel, Stage 1 converges to SSD (depicted by the dotted black line). On the top-right panel, we examine the transient dynamics by considering two stages. We follow the convergence to SSD with Stage 5 on the x-axis and Stage 1 on the y-axis. The bottom two panels follow transient dynamics in Stage 1 after a press disturbance to two elements of the transition matrix (with 6 stages). We perturb (1,5) and (5,6) elements of the MP and follow the convergence to SSD for Stage 1. As shown in bottom-left panel, Stage 1 is perturbed from its SSD (depicted by dotted black line) and converges to a new SSD (depicted by the dashed black line) following a press disturbance. On the bottom-right panel, we examine the transient dynamics by considering two stages, Stage 1 on the y-axis and Stage 5 on the x-axis. Picture credit for *Phaseolus lunatus*: iNaturalist

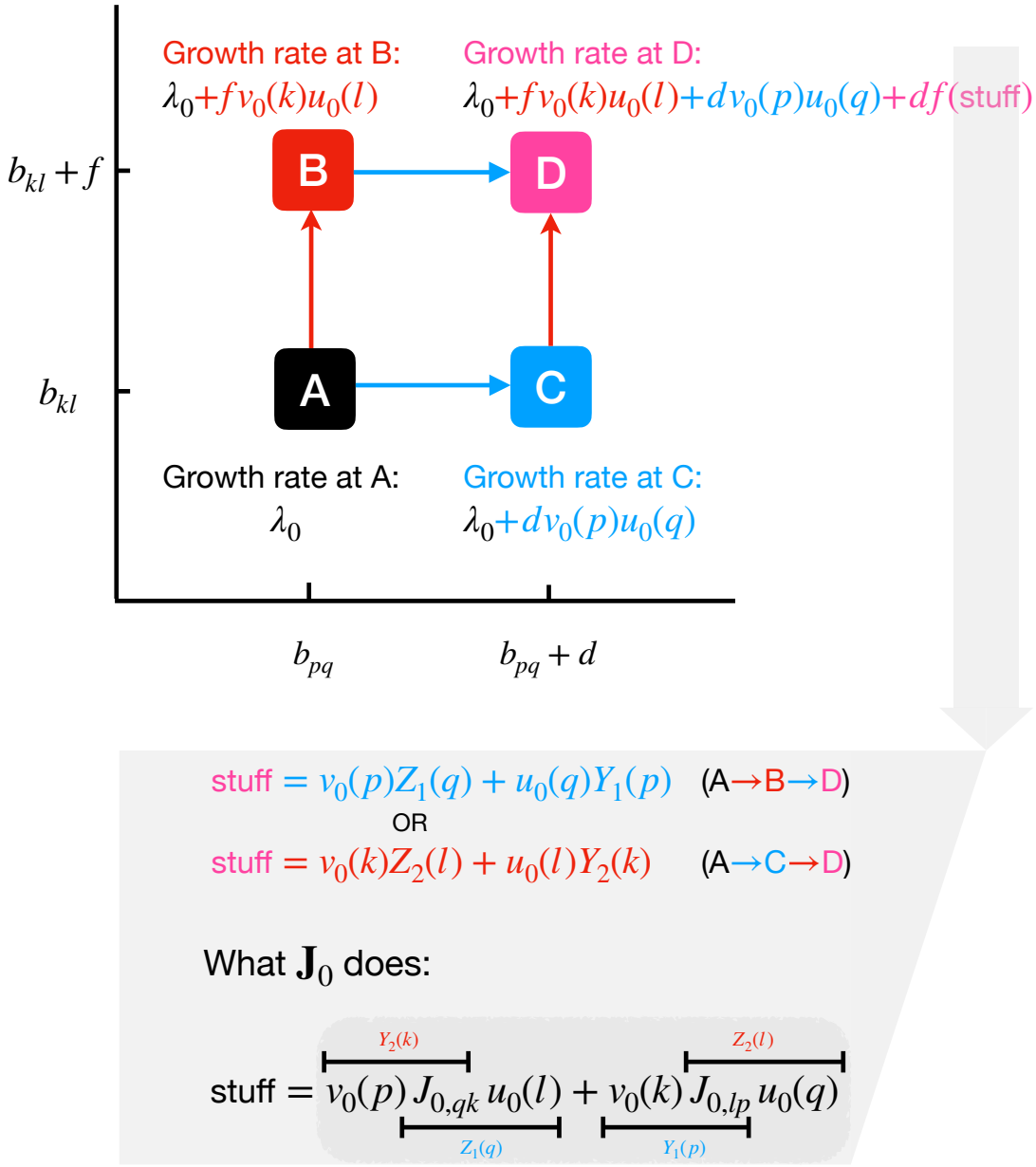

Figure 4: Computing the second derivatives of fitness with respect to projection matrix elements. The horizontal and vertical axes indicate rates for the two demographic transitions, (p, q) and (k, l). Point A indicates the starting values, where the fitness is λ_0, SSD is $\mathbf{u}_0$ and stable reproductive value is $\mathbf{v}_0$. A press disturbance of both demographic rates ends at point D. We consider two possible routes. First route: go from A to B by changing only the demographic rate for the $k \leftarrow l$ transition (*i.e.*, b_{pq} is unchanged but b_{kl} becomes $b_{kl} + f$. At B the new stable population is, say, $\mathbf{u}_0 + f\mathbf{Z}_1$ and the new reproductive value is, say, $\mathbf{v}_0 + f\mathbf{Y}_1$. Next go from B to D, by changing only b_{pq} by an amount d. Second route: starting at A, go from A to C by perturbing the $p \leftarrow q$ transition rate by an amount d. At C the new stable population is, say, $\mathbf{u}_0 + d\,\mathbf{Z}_2$ and the new reproductive value is, say, $\mathbf{v}_0 + d\,\mathbf{Y}_2$. Next, go from C to D by changing only b_{kl} by an amount f.

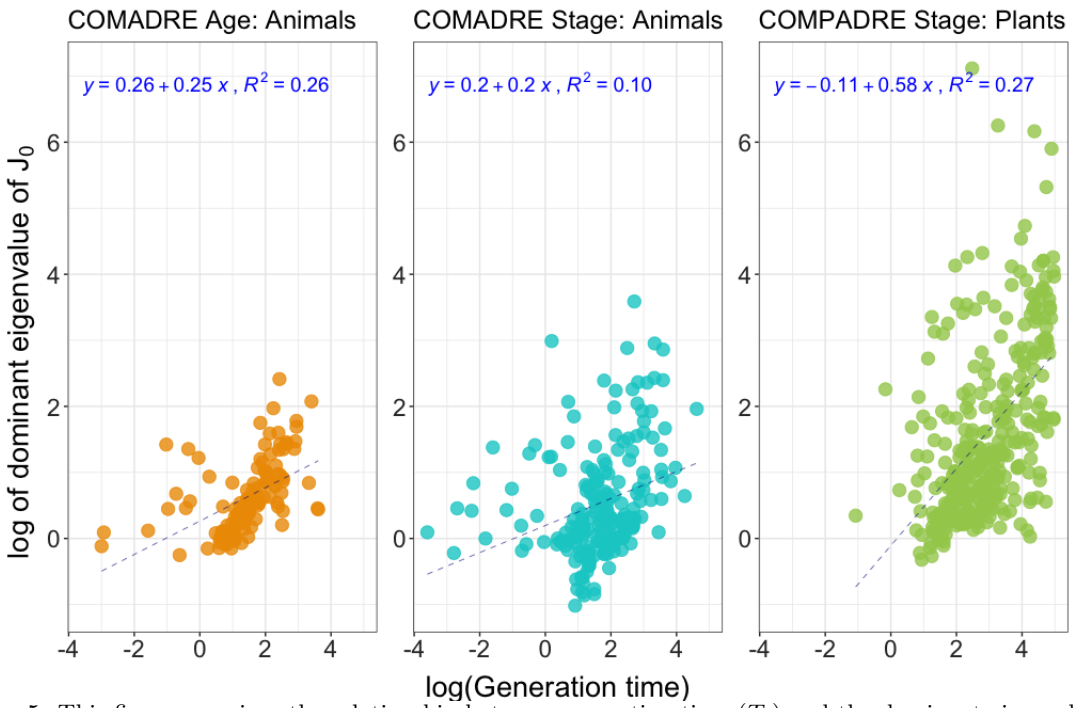

Figure 5: This figure examines the relationship between generation time (T_c) and the dominant eigenvalue of $\mathbf{J}_0$ based on phylogenetic generalized least squares. The y-axis corresponds to log of the dominant eigenvalue of $\mathbf{J}_0$ and the x-axis corresponds to log of generation time T_c. Each panel corresponds to a database: COMADRE age-structured matrices, COMADRE stage-structured matrices, COMPADRE stage-structured matrices. The correlation between dominant eigenvalue of $\mathbf{J}_0$ and T_c is consistently positive across all databases.

Appendix

1 Pulse Disturbances and Transients

Basic Decomposition

The stability of the population structure means that the perpendicular component $\mathbf{u}_\perp$ goes to zero over time. This is because if $u_\perp$ was parallel to $\mathbf{u}_0$, the new stable structure would simply be a multiple of the original. We can express this concept by decomposing $\mathbf{B}$ as a sum of two matrices (as discussed in the main text) such that $\mathbf{B} = \mathbf{Q}_0 + \mathbf{Q}_1$ where:

$$\mathbf{Q}_0 = \mathbf{u}_0\,\mathbf{v}_0^T, \text{ and } \mathbf{Q}_1 = \frac{1}{\lambda_0}\left(\mathbf{B} - \lambda_0\,\mathbf{Q}_0\right) \tag{A.1}$$

Here, $\mathbf{Q}_0$ is a projection matrix, *i.e.*, $\mathbf{Q}_0^2 = \mathbf{Q}_0$ and $\mathbf{Q}_0$, $\mathbf{Q}_1$ are orthogonal to each other ($\mathbf{Q}_1\,\mathbf{Q}_0 = \mathbf{Q}_0\mathbf{Q}_1 = 0$). Starting from the initial $t = 0$ and moving to a later $t > 0$ means we follow

$$\begin{aligned}
\mathbf{B}^t &= \lambda_0^t\left(\mathbf{Q}_0^t + \mathbf{Q}_1^t\right)\\
\mathbf{B}^t &= \lambda_0^t\left(\mathbf{Q}_0 + \mathbf{Q}_1^t\right)\\
\frac{\mathbf{B}^t\mathbf{n}(0)}{\lambda_0^t} &= \left(\mathbf{Q}_0 + \mathbf{Q}_1^t\right)\mathbf{n}(0)\\
\frac{\mathbf{n}(t)}{\lambda_0} &= \left(\mathbf{Q}_0 + \mathbf{Q}_1^t\right)\mathbf{n}(0)
\end{aligned}$$

As shown by, Karlin and Taylor (1975), equation 4 implies that the powers of $\mathbf{Q}_1$ must be getting small, *i.e.*, $\mathbf{Q}_1^t \to 0$ time t becomes large. Thus, stability means that the second term on the right goes to zero and the powers of $\mathbf{Q}_1$ describe the transient dynamics of the population.

In terms of pulse disturbance, at time 0, one time shock $\mathbf{u}_\perp$ acts on stable stage distribution $\mathbf{u}_0$ (of population matrix $\mathbf{B}/\lambda_0$ (scaled by growth rate)) to give the new stage distribution $\mathbf{B}\left(\mathbf{u}_0 + \mathbf{u}_\perp\right)/\lambda_0$. At time 1, stage distribution is $\mathbf{u}_0 + \mathbf{Q}_1\mathbf{u}_\perp$, at time 2, the stage distribution is $\mathbf{u}_0 + \mathbf{Q}_1^2\mathbf{u}_\perp$ and so on. After t time steps, $\mathbf{u}_0 + \mathbf{Q}_1^t\mathbf{u}_\perp$ eventually converges to $\mathbf{u}_0$ as illustrated in the left panels of Figure 1 and 2.

2 Perturbation Theory: Press as Accumulated Pulses

Our analysis follows the perturbation approach in Chapter 2 of Kato (1976). We examine the effects of changing the matrix $\mathbf{B}$ by a small amount to $\mathbf{B} + \epsilon\mathbf{D}$. Since ϵ is small, we only need $\mathbf{D}$ (as defined in the main text) to be finite. For example, to examine only the effects of a small change in an element of $\mathbf{B}$, only the corresponding element of $\mathbf{D}$ would be non-zero and equal to 1. Below we use power series in ϵ for the derivation.

A disturbance in the matrix elements of $\mathbf{B}$ at time t_0 will produce changes in the dominant eigen-

value and corresponding right eigenvector (in the next time t_1) as,

$$\lambda(\epsilon) = \lambda_0 + \epsilon\,\eta_1 + \epsilon^2\,\eta_2 + O(\epsilon^3), \tag{A.2}$$

$$u(\epsilon) = \mathbf{u}_0 + \epsilon\,\mathbf{z}_1 + \epsilon^2\,\mathbf{z}_2 + O(\epsilon^3), \tag{A.3}$$

so that

$$(\mathbf{B} + \epsilon\mathbf{D})\,(\mathbf{u}_0 + \epsilon\,\mathbf{z}_1 + \epsilon^2\,\mathbf{z}_2) = (\lambda_0 + \epsilon\,\eta_1 + \epsilon^2\,\eta_2)\,(\mathbf{u}_0 + \epsilon\,\mathbf{z}_1 + \epsilon^2\,\mathbf{z}_2). \tag{A.4}$$

Multiplying through in equation (A.4) and collecting terms in $\epsilon^0, \epsilon^1, \epsilon^2$ leads to three equations,

$$\mathbf{B}\mathbf{u}_0 = \lambda_0\,\mathbf{u}_0, \tag{A.5}$$

$$\mathbf{B}\mathbf{z}_1 + \mathbf{D}\mathbf{u}_0 = \lambda_0\mathbf{z}_1 + \eta_1\mathbf{u}_0, \tag{A.6}$$

$$\mathbf{B}\mathbf{z}_2 + \mathbf{D}\mathbf{z}_1 = \lambda_0\mathbf{z}_2 + \eta_1\mathbf{z}_1 + \eta_2\mathbf{u}_0. \tag{A.7}$$

The first of these is obviously true. The others must be used to find the perturbations – the subject of classical perturbation theory. The first-order effects in the middle equation (A.6) yield the first derivatives of λ_0 and have been applied in ecology Caswell (1996, 2001b) to study sensitivity and elasticity.

A key point is that $\mathbf{z}_1$ and $\mathbf{z}_2$ must be perpendicular to $\mathbf{u}_0$ – if not we will just multiply both $\mathbf{B}$ and $\mathbf{u}_0$ by the same factor.Mathematically we require that $\mathbf{z}_1$ and $\mathbf{z}_2$ are orthogonal to $\mathbf{u}_0$ and so,

$$0 = (\mathbf{v}_0, \mathbf{z}_1) = (\mathbf{v}_0, \mathbf{z}_2), \tag{A.8}$$

$$0 = \mathbf{Q}_0\mathbf{z}_1 = \mathbf{Q}_0\mathbf{z}_2, \tag{A.9}$$

$$\mathbf{z}_1 = (\mathbf{I} - \mathbf{Q}_0)\,\mathbf{z}_1. \tag{A.10}$$

A.1 First Order Perturbation: finding η_1

Multiply equation (A.6) by $\mathbf{v}_0^\dagger$ (where † means transpose and conplex conjugate) on the left to see that

$$\mathbf{v}_0^\dagger(\mathbf{B}\mathbf{z}_1 + \mathbf{D}\mathbf{u}_0) = \mathbf{v}_0^\dagger(\lambda_0\mathbf{z}_1 + \eta_1\mathbf{u}_0)$$

$$\mathbf{v}_0^\dagger\mathbf{B}\mathbf{z}_1 + \mathbf{v}_0^\dagger\mathbf{D}\mathbf{u}_0 = \lambda_0\mathbf{v}_0^\dagger\mathbf{z}_1 + \eta_1\mathbf{v}_0^\dagger\mathbf{u}_0$$

$$\cancel{\lambda_0\mathbf{v}_0^\dagger\mathbf{z}_1} + \mathbf{v}_0^\dagger\mathbf{D}\mathbf{u}_0 = \cancel{\lambda_0\mathbf{v}_0^\dagger\mathbf{z}_1} + \eta_1$$

Thus,

$$\eta_1 = \mathbf{v}_0^\dagger\mathbf{D}\,\mathbf{u}_0, \tag{A.11}$$

$$= \sum_i \sum_j v_{0i}\mathbf{D}_{ij}u_{0j}. \tag{A.12}$$

This is first-order perturbation (coefficient of ϵ in equation (A.7)). Following Caswell, take the

(i, j) element of $\mathbf{D}$ to be 1 ($d_{ij} = 0$) and all other elements to be zero, thus yielding the sensitivity

$$v_{0i}\, u_{0j} = \frac{\partial \lambda_0}{\partial b_{ij}} = s_{ij}. \tag{A.13}$$

A.2 Second Order Perturbation: finding η_2

Second-order perturbations yield η_2. Similar to first-order perturbation, multiply equation (A.6) by $\mathbf{v}_0^\dagger$ on the left and use the orthogonality discussed above (A.8) to see that

$$\eta_2 = \mathbf{v}_0^\dagger \mathbf{D}\, \mathbf{z}_1. \tag{A.14}$$

Note that η_2 is a nonlinear response (coefficient of ϵ^2 in equation (A.7)). So far, $\mathbf{z}_1$ is unknown. To get $\mathbf{z}_1$, we first use the following relation:

$$\begin{aligned}
(\mathbf{I} - \mathbf{Q}_0)\, \mathbf{B}\mathbf{z}_1 &= \mathbf{B}\mathbf{z}_1 - \mathbf{Q}_0\mathbf{B}\mathbf{z}_1 \\
&= \mathbf{B}\mathbf{z}_1 - \mathbf{u}_0\mathbf{v}_0^\top \mathbf{B}\mathbf{z}_1 \\
&= \mathbf{B}\mathbf{z}_1 - \lambda_0\mathbf{u}_0\mathbf{v}_0^\top \mathbf{z}_1 \\
&= \mathbf{B}\mathbf{z}_1 - \lambda_0\mathbf{Q}_0\mathbf{z}_1 \\
&= (\mathbf{B} - \lambda_0\mathbf{Q}_0)\, \mathbf{z}_1 \\
&= \lambda_0\mathbf{Q}_1\mathbf{z}_1
\end{aligned}$$

Also, $(\mathbf{I} - \mathbf{Q}_0)\, \mathbf{u}_0 = 0$ because scalar product of $\mathbf{u}_0$ and $\mathbf{v}_0$ is 1. Using the previous two expressions, multiplying equation (A.6) by $(\mathbf{I} - \mathbf{Q}_0)$ on the left and comparing the coefficients on both sides of equation (A.6) we get:

$$\lambda_0\mathbf{Q}_1\mathbf{z}_1 + (\mathbf{I} - \mathbf{Q}_0)\mathbf{D}\mathbf{u}_0 = \lambda_0\mathbf{z}_1.$$

This yields

$$\mathbf{z}_1 = \frac{1}{\lambda_0}(\mathbf{I} - \mathbf{Q}_1)^{-1}\, (\mathbf{I} - \mathbf{Q}_0)\mathbf{D}\mathbf{u}_0. \tag{A.15}$$

Note that as illustrated in Figure 2 and in the main text, $\mathbf{z}^* = (\mathbf{I} - \mathbf{Q}_0)\mathbf{D}\mathbf{u}_0/\lambda_0$ and so,

$$\mathbf{z}_1 = (\mathbf{Q}_1 + \mathbf{Q}_1^2 + \mathbf{Q}_1^3 + \cdots)\mathbf{z}^* \tag{A.16}$$

$$= (\mathbf{I} - \mathbf{Q}_1)^{-1}\mathbf{z}^*. \tag{A.17}$$

Note that in the main text $\mathbf{Z} = (\mathbf{I} - \mathbf{Q}_1)^{-1} z^* = \mathbf{z}_1$.

Substitute the value of $\mathbf{z}_1$ (from equation (A.15)) in equation (A.14) to get

$$\eta_2 = \frac{1}{\lambda_0}\mathbf{v}_0^\dagger \mathbf{D}\, (\mathbf{I} - \mathbf{Q}_1)^{-1}\, (\mathbf{I} - \mathbf{Q}_0)\mathbf{D}\mathbf{u}_0. \tag{A.18}$$

We define a matrix $\mathbf{J}_0$ such that

$$\mathbf{J}_0 = \frac{1}{\lambda_0}(\mathbf{I} - \mathbf{Q}_1)^{-1}(\mathbf{I} - \mathbf{Q}_0). \tag{A.19}$$

Finally, the second order coefficient can be written as:

$$\eta_2 = \mathbf{v}_0^\dagger \mathbf{D}\, \mathbf{J}_0 \mathbf{D}\mathbf{u}_0. \tag{A.20}$$

A.3 Second order derivatives

Given the above disturbance for some matrix $\mathbf{D}$, we can write the change in the dominant eigenvalue as a Taylor series:

$$\lambda(\mathbf{B} + \epsilon\mathbf{D}) = \lambda_0 \tag{A.21}$$

$$+ \epsilon \sum_{ij} \mathbf{D}_{ij} \frac{\partial \lambda_0}{\partial b_{ij}} \tag{A.22}$$

$$+ \frac{1}{2}\epsilon^2 \sum_{ij}\sum_{mn} \mathbf{D}_{ij}\, \mathbf{D}_{mn} \frac{\partial^2 \lambda_0}{\partial b_{ij} \partial b_{mn}}. \tag{A.23}$$

Using this expansion for $\lambda(\mathbf{B} + \epsilon\mathbf{D}) + \lambda(\mathbf{B} - \epsilon\mathbf{D})$, the first-order term (in ϵ) cancels out to give:

$$\lambda(\mathbf{B} + \epsilon\mathbf{D}) - \lambda_0 + \lambda(\mathbf{B} - \epsilon\mathbf{D}) - \lambda_0 = \epsilon^2 \sum_{ij}\sum_{mn} \mathbf{D}_{ij}\, \mathbf{D}_{mn} \frac{\partial^2 \lambda_0}{\partial b_{ij} \partial b_{mn}}$$

Given equation (A.2) and substituting the expression for η_2 in equation (A.20) we get

$$2\,\eta_2 = \sum_{ij}\sum_{mn} \mathbf{D}_{ij}\, \mathbf{D}_{mn} \frac{\partial^2 \lambda_0}{\partial b_{ij} \partial b_{mn}}. \tag{A.24}$$

$$2\,\eta_2 = 2\,\mathbf{v}_0^\dagger \mathbf{D}\mathbf{J}_0\mathbf{D}\mathbf{u}_0 = 2\sum_{ij}\sum_{mn} v_{0i}\mathbf{D}_{ij}\mathbf{J}_{jm}\mathbf{D}_{mn}u_{0n}, \tag{A.25}$$

where we've used the double-index-sum and so are summing over i, j, m, n. Let us first perturb only element (p, q), so the only nonzero element of $\mathbf{D}$ is d_{pq}. In that case the sum in equation (A.25) simplifies to yield

$$2\,\eta_2(pq, pq) = 2\, v_{0p}\mathbf{J}_{qp}u_{0q}. \tag{A.26}$$

We use (pq, pq) on the left to indicate that only that element is being perturbed, and this a second-order effect. So in that case equation (A.24) implies that

$$\frac{\partial^2 \lambda_0}{\partial b_{pq} \partial b_{pq}} = 2\,\eta_2(pq, pq). \tag{A.27}$$

Now perturb distinct elements p, q and k, l, so in (A.25) we write

$$\mathbf{D}_{ij} = \delta_{ip}\delta_{jq} + \delta_{ik}\delta_{jl}, \tag{A.28}$$

$$\mathbf{D}_{mn} = \delta_{mp}\delta_{nq} + \delta_{mk}\delta_{nl}, \tag{A.29}$$

where we use Kronecker deltas defined as $\delta_{ij} = \begin{cases} 0 & \text{if } i \neq j, \\ 1 & \text{if } i = j. \end{cases}$

Now the sums in (A.25) lead to 4 terms,

$$2\,\eta_2(pq, kl) = 2\Big[v_{0p}\mathbf{J}_{qp}u_{0q} + \quad v_{0p}\mathbf{J}_{qk}u_{0l} + v_{0k}\mathbf{J}_{lp}u_{0q} + \quad + v_{0k}\mathbf{J}_{lk}u_{0l}\Big]. \tag{A.30}$$

From (A.25) and (A.27) we conclude that

$$2\,\eta_2(pq, kl) = \frac{\partial^2\lambda_0}{\partial b_{pq}\partial b_{pq}} \quad + \frac{\partial^2\lambda_0}{\partial b_{pq}\partial b_{kl}} \quad + \frac{\partial^2\lambda_0}{\partial b_{kl}\partial b_{pq}} + \quad \frac{\partial^2\lambda_0}{\partial b_{kl}\partial b_{kl}}. \tag{A.31}$$

Therefore,

$$\boxed{\frac{\partial^2\lambda_0}{\partial b_{pq}\partial b_{kl}} = v_{0p}\mathbf{J}_{qk}u_{0l} + v_{0k}\mathbf{J}_{lp}u_{0q}} \tag{A.32}$$

We can define the sensitivities, $s_{pl} = v_{0p}\,u_{0l}$ and rewrite the above expression on the right-hand side as: $[s_{pl}\,J_{0,qk} + s_{kq}\,J_{0,lp}]$ and hence in terms of kronecker-product the expression simplifies to

$$\boxed{\frac{\partial^2\lambda_0}{\partial b_{pq}\partial b_{kl}} = \big[\mathbf{S}\otimes\mathbf{J}^T + \mathbf{J}^T\otimes\mathbf{S}\big]_{pl,kq}} \tag{A.33}$$

A.4 Getting to the hessian - the matrix of second derivatives

Here we construct a matrix, Hessian ($\mathbf{H}$), to place all the second derivatives calculated from equation (A.32). Suppose the population matrix $\mathbf{B}$ is $S \times S$. Then define indices x, y that take values $1, 2, \ldots, S^2$. We list the elements of $\mathbf{B}$ columnwise which gives a vector $\mathbf{b}$, so $b_{pq} \equiv \mathbf{b}_x$ with

$$x = p + (q-1)S, \tag{A.34}$$

Therefore,

$$\mathbf{H}_{xy} = \frac{\partial^2\lambda_0}{\partial b_{pq}\partial b_{kl}}, \tag{A.35}$$

where $x = p + (q-1)S$ and $y = k + (l-1)S$.

A.5 The Second derivatives for *Phaseolus lunatus*

The matrix for *Phaseolus lunatus* is

$$\mathbf{B} = \begin{pmatrix} 0.00 & 0.00 & 0.00 & 0.42 & 28.90 & 104.00 \\ 0.16 & 0.00 & 0.00 & 0.00 & 0.00 & 0.00 \\ 0.12 & 0.14 & 0.00 & 0.00 & 0.00 & 0.00 \\ 0.08 & 0.09 & 0.01 & 0.01 & 0.00 & 0.00 \\ 0.00 & 0.00 & 0.00 & 0.05 & 0.16 & 0.00 \\ 0.00 & 0.00 & 0.00 & 0.00 & 0.18 & 0.25 \end{pmatrix}$$

$$\mathbf{u}_0 = \begin{pmatrix} 0.645 \\ 0.134 \\ 0.125 \\ 0.086 \\ 0.007 \\ 0.002 \end{pmatrix} \;\&\; \mathbf{v}_0 = \begin{pmatrix} 0.373 \\ 0.340 \\ 0.037 \\ 2.842 \\ 39.929 \\ 74.918 \end{pmatrix}$$

$$\mathbf{J}_0 = \begin{pmatrix} 0.5573 & -0.6256 & -0.0675 & -2.7940 & -10.3566 & 18.6310 \\ 0.0509 & 1.1128 & -0.0206 & -1.0802 & -9.1522 & -9.2380 \\ 0.0355 & 0.0497 & 1.2824 & -1.0979 & -9.8089 & -11.0066 \\ 0.0232 & 0.0283 & 0.0032 & 0.5605 & -6.8290 & -7.7534 \\ -0.0024 & -0.0016 & -0.0002 & 0.0131 & 0.6202 & -1.5080 \\ -0.0026 & -0.0022 & -0.0002 & -0.0089 & 0.0264 & 1.0525 \end{pmatrix}$$

To obtain the second derivative of growth rate, we need the marginal effect of perturbing two demographic rates. For ease of exposition, say we make a press disturbance and change the $(1, 5)$ and $(6, 5)$ matrix elements to $b_{15} + 23.12$ and $b_{65} + 0.144$, where the change $d = 23.12$ and $f = 0.144$.

Fig A.1 illustrates two distinct ways of carrying out the above press disturbance, which must lead to the same overall change in fitness. Say we use the first route, A to B and then B to D. In the change from A to B, our simple argument above shows that the change in fitness is the product

$$f\, v_0[6]\, u_0[5] = 0.144 \times 74.9 \times 0.007 = 0.076. \tag{A.36}$$

Now we want to make the change from B to D. But at B, equation (9) shows that the SSD has already changed to $(\mathbf{u}_0 + f\,\mathbf{Z}_1)$ with

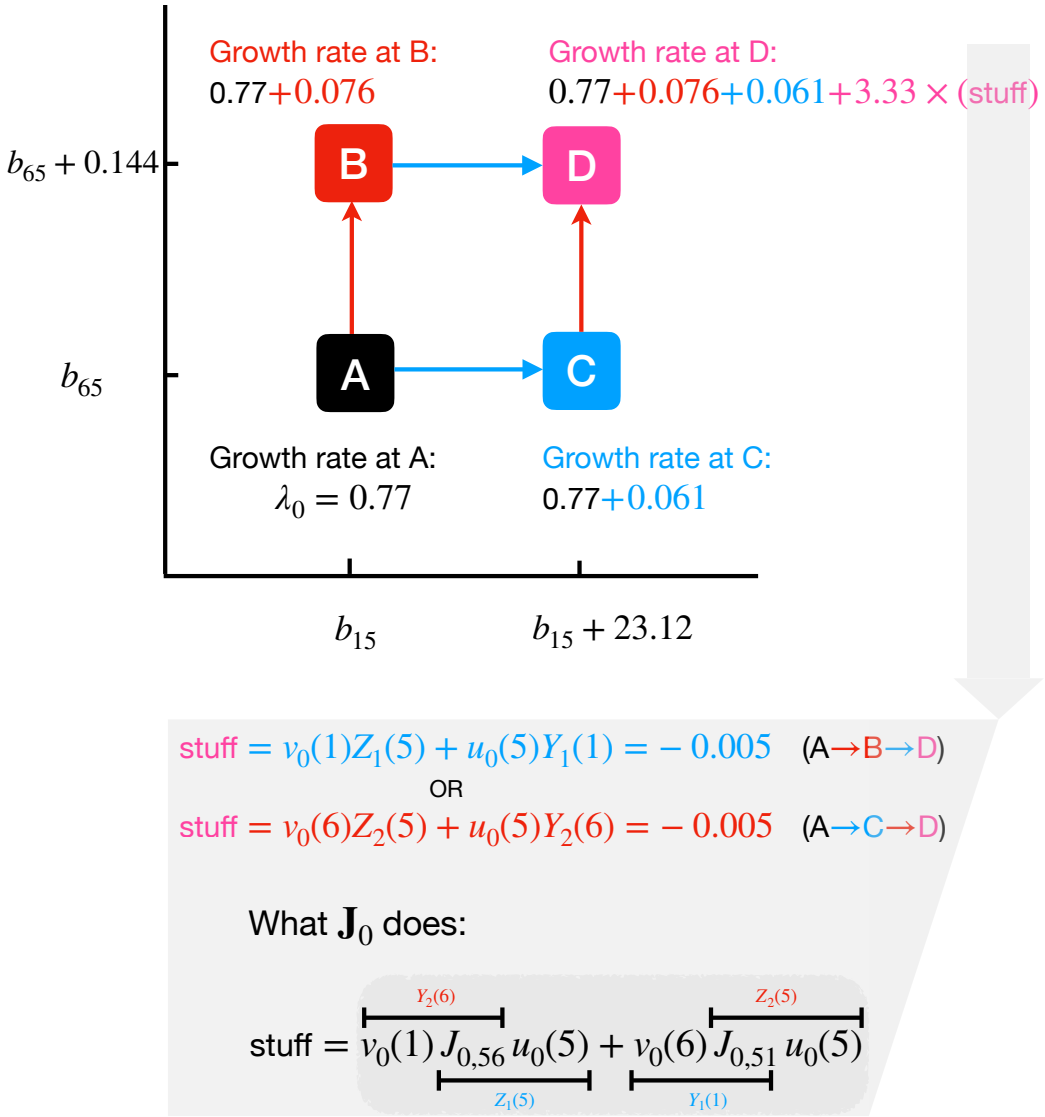

Figure A.1: Computing the second derivatives of fitness with respect to projection matrix elements. The horizontal and vertical axes indicate rates for the two demographic transitions, $[1,5]$ and $[6,5]$. Point A indicates the starting values, where the fitness is $\lambda_0 = 0.77$, SSD is $\mathbf{u}_0$ and stable reproductive value is $\mathbf{v}_0$. A press disturbance of both demographic rates ends at point D. We consider two possible routes. First route: go from A to B by changing only the demographic rate for the $6 \leftarrow 5$ transition (*i.e.*, b_{15} is unchanged but b_{65} becomes $b_{65}+0.144$. At B the new stable population is, say, $\mathbf{u}_0 + 0.144\mathbf{Z}_1$ and the new reproductive value is, say, $\mathbf{v}_0 + 0.144\mathbf{Y}_1$. Next go from B to D, by changing only b_{15} by an amount 23.12. Second route: starting at A, go from A to C by perturbing the $1 \leftarrow 5$ transition rate by an amount 23.12. At C the new stable population is, say, $\mathbf{u}_0 + 23.12\,\mathbf{Z}_2$ and the new reproductive value is, say, $\mathbf{v}_0 + 23.12\,\mathbf{Y}_2$. Next, go from C to D by changing only b_{56} by an amount 0.144.

$$\mathbf{Z}_1 = u_0[5]\begin{pmatrix} J_{0,16} \\ J_{0,26} \\ J_{0,36} \\ J_{0,46} \\ J_{0,56} \end{pmatrix} = 0.007 \times \begin{pmatrix} 18.6 \\ -9.2 \\ -11.0 \\ -7.8 \\ -1.5 \end{pmatrix} = \begin{pmatrix} 0.13 \\ -0.06 \\ -0.08 \\ -0.05 \\ -0.01 \end{pmatrix}. \tag{A.37}$$

Also at B, equation (10) shows that the stable reproductive value has also already changed to $(\mathbf{v}_0 + f\,\mathbf{Y}_1)$ with

$$\begin{aligned}\mathbf{Y}_1^T &= v_0[6]\,\begin{pmatrix} J_{0,51} & J_{0,52} & J_{0,53} & J_{0,54} & J_{0,55} & J_{0,56}\end{pmatrix}\\ &= 74.92\times\begin{pmatrix} -0.0024 & -0.0016 & -0.0002 & 0.0131 & 0.6202 & -1.5080\end{pmatrix}\\ &= \begin{pmatrix} -0.2 & -0.1 & 0.0 & 1.0 & 46.5 & -113.0\end{pmatrix}.\end{aligned} \tag{A.38}$$

Now we are ready to use our approach to say that in the transition B to D, the fitness changes by the product of

a) the stable proportion in stage 5, which equation (A.37) shows is $(u_0[5] + fZ_1(5)) = 0.006$,

b) the change in the rate, $d = 23.12$,

c) the stable reproductive value in stage 1, which equation (A.38) shows is $(v_0[1] + fY_1(1)) = 0.347$.

The product of these terms has to be added to the change (equation (A.36)) to get the total change in growth rate A to B to D,

$$f\,v_0[6]\,u_0[5] + d\,v_0[1]\,u_0[5] + f\,d\,\left(u_0[5]\,Y_1(1) + v_0[1]Z_1(5)\right) = 0.119. \tag{A.39}$$

Using (A.37 – A.38) the total change is the sum

$$\begin{aligned}\text{Linear change} &= f\,v_0[6]\,u_0[5] + d\,v_0[1]\,u_0[5] = 0.14,\\ &+\\ \text{Nonlinear change} &= f\,d\,\left(u_0[5]\,v_0[6]\,J_{0,15} + u_0[5]\,v_0[1]\,J_{0,56}\right) = -0.017.\end{aligned} \tag{A.40}$$

As shown in Fig A.1, we could alternatively go from A to C and then C to D. That process involves distinct changes to the SSD and reproductive value. But we get the same final result as in equation (A.40).

We conclude that the nonlinearity is revealed by making two press disturbances. Think about these changes in terms of the second derivatives of fitness to find

$$\frac{\partial^2\lambda_0}{\partial b_{15}\partial b_{65}} = \left[s_{15}\,J_{0,56} + s_{65}\,J_{0,51}\right] = -0.005 \tag{A.41}$$

where we have used the sensitivities equation (11). Note that our expression for the second derivative is symmetric with respect to an exchange of the elements b_{15}, b_{65} (as it should be).

The curvature of fitness as measured by the second derivatives in equation (**??**) depends on the matrix $\mathbf{J}_0$. Consequently any analysis of second derivatives will provide detailed information about $\mathbf{J}_0$. The next section describes the many connections between $\mathbf{J}_0$ and transient dynamics.

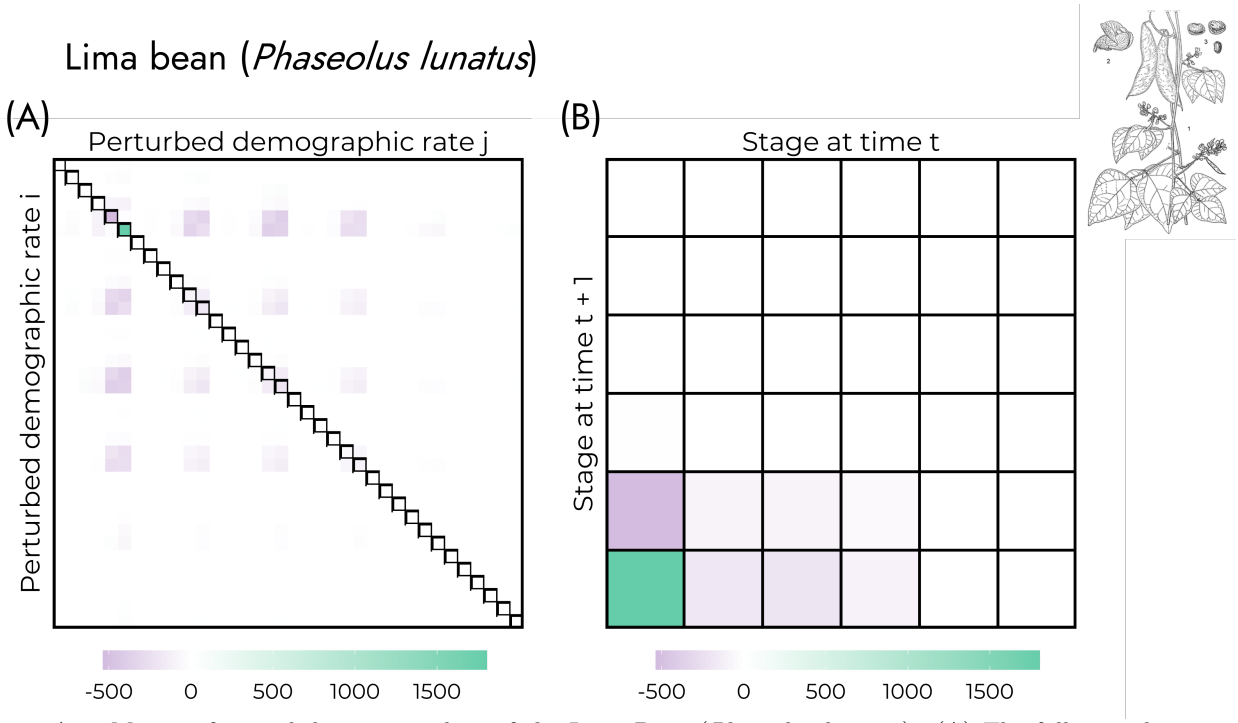

Figure A.2: Matrix of second derivative values of the Lima Bean (*Phaseolus lunatus*). (A) The full second derivative matrix. The self-second derivatives are situated along with main diagonal and visualized with a black border. (B) Isolated self-second derivatives. Purple means negative value, whereas green positive.

A.6 An example for comparison with Shyu and Caswell (2014): evaluating second derivatives

We compute the second derivatives to show that our method yields the same result as the one in Shyu and Caswell (2014). The example is an 8×8 stage-structured matrix for *Calathea ovandensis*, a neotropical perennial herb that inhabits forest understories. The matrix was originally developed by Horvitz and Schemske (1995) and contains eight stages distinguished by size and reproductive ability: seeds, nonreproductive stages (seedlings, juveniles, pre-reproductive), and reproductive stages (small, medium, large and extra large).

The transition matrix is:

$$A = \begin{pmatrix} 0.4983 & 0 & 0.5935 & 7.139 & 14.2715 & 24.6953 & 34.9027 & 40.5437 \\ 0.0973 & 0.0110 & 0.0191 & 0 & 0 & 0 & 0 & 0 \\ 0.0041 & 0.0442 & 0.3378 & 0.0698 & 0.0251 & 0.0065 & 0.0085 & 0 \\ 0 & 0.0014 & 0.1355 & 0.4286 & 0.1736 & 0.0968 & 0.0427 & 0.0435 \\ 0 & 0 & 0.0363 & 0.3841 & 0.6025 & 0.4258 & 0.2991 & 0.2174 \\ 0 & 0 & 0.0019 & 0.0254 & 0.113 & 0.2387 & 0.1709 & 0.2826 \\ 0 & 0 & 0 & 0.0095 & 0.0272 & 0.1548 & 0.3248 & 0.1957 \\ 0 & 0 & 0 & 0.0032 & 0.0063 & 0.0452 & 0.1282 & 0.2391 \end{pmatrix}.$$

In this example, the matrix of second order derivatives of λ_0 with respect to elements b_{pq}, b_{kl} of A is

a 64×64 symmetric matrix. To calculate the second derivatives, we find the dominant eigenvalue and corresponding eigenvector (normalized) of A and use this to get the orthogonal matrices $\mathbf{Q}_0$ and $\mathbf{Q}_1$. The dominant eigenvalue here is 0.9923 and indicates a near-steady state population. Next, we can easily evaluate the matrix $\mathbf{J}_0$ and run a loop for all pairs (p, q) and (k, l) to arrive at the same 64×64 symmetric matrix of second-derivatives as Shyu and Caswell (2014). We can reduce computational runtime by running the loop only over elements for upper (or lower) triangle of the matrix.

3 Relation between $\mathbf{J}_0$ and Cohen's cumulative distance

$$
\begin{aligned}
\mathbf{J}_0 - \mathbf{D}_1 &= (\mathbf{I} - \mathbf{Q}_1)^{-1} (\mathbf{I} - \mathbf{Q}_0) - (\mathbf{I} - \mathbf{Q}_1)^{-1} + \mathbf{Q}_0 \\
&= (\mathbf{I} - \mathbf{Q}_1)^{-1} (\mathbf{I} - \mathbf{Q}_0 - \mathbf{I}) + \mathbf{Q}_0 \\
&= \mathbf{Q}_0 - \mathbf{Q}_0 (\mathbf{I} - \mathbf{Q}_1)^{-1} \\
&= \mathbf{Q}_0 (\mathbf{I} - \mathbf{Q}_1) (\mathbf{I} - \mathbf{Q}_1)^{-1} - \mathbf{Q}_0 [\mathbf{I} - \mathbf{Q}_1)^{-1} \\
&= ((\mathbf{I} - \mathbf{Q}_1) \mathbf{Q}_0 - \mathbf{Q}_0) (\mathbf{I} - \mathbf{Q}_1)^{-1} \\
&= (\mathbf{Q}_0 - \mathbf{Q}_1 \mathbf{Q}_0 - \mathbf{Q}_0) (\mathbf{I} - \mathbf{Q}_1)^{-1} \\
&= 0 \text{ (because } \mathbf{Q}_1 \mathbf{Q}_0 \text{ are orthogonal as discussed above)}
\end{aligned}
$$

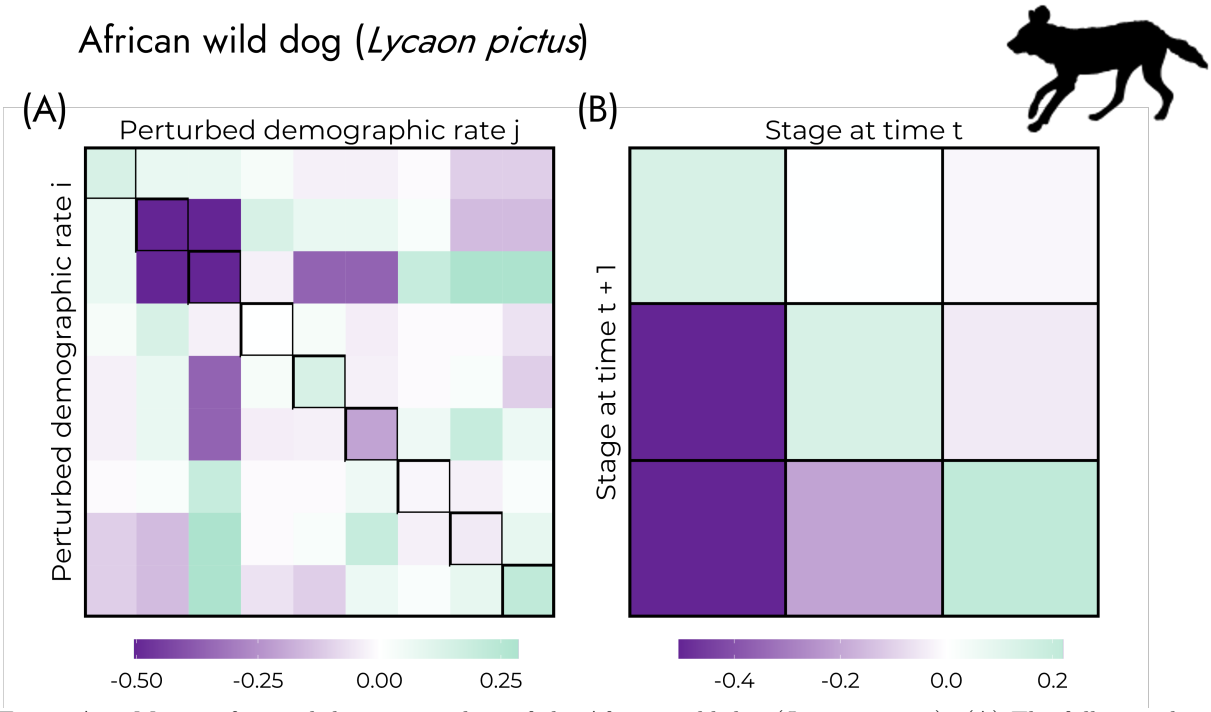

Figure A.3: Matrix of second derivative values of the African wild dog (*Lycaon pictus*). (A) The full second derivative matrix. The self-second derivatives are situated along with main diagonal and visualized with a black border. (B) Isolated self-second derivatives. Purple means negative value, whereas green positive.

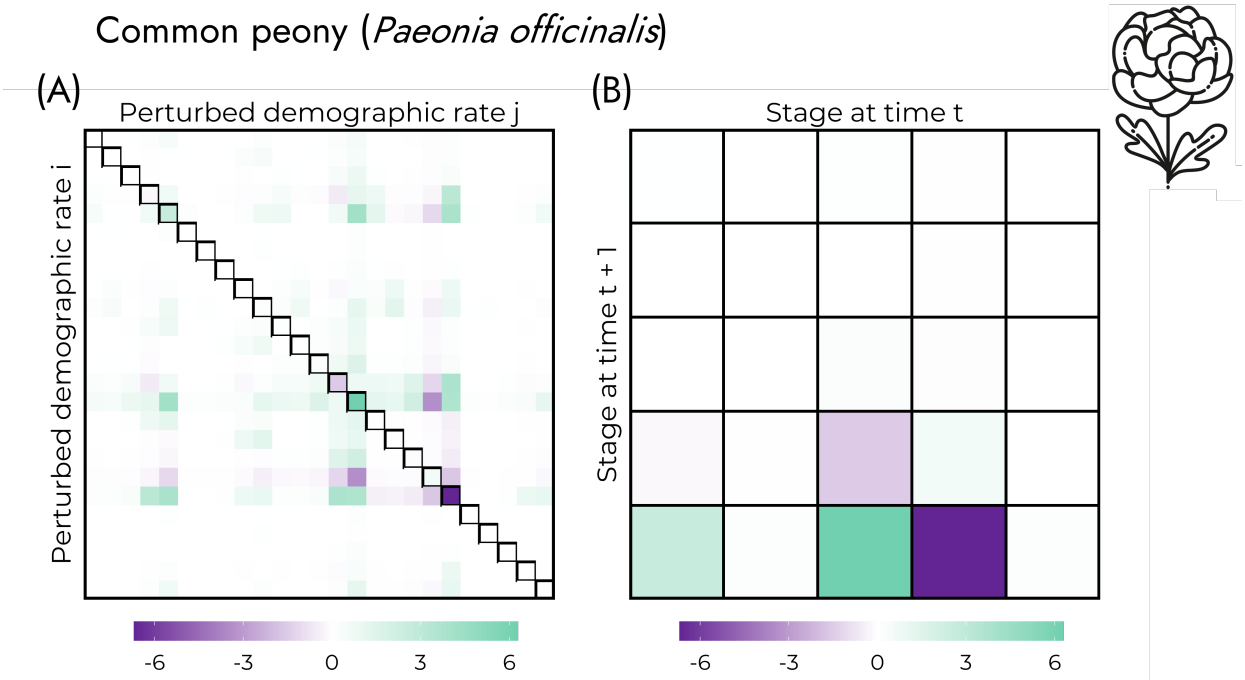

Figure A.4: Matrix of second derivative values of the common peony (*Paeonia officinalis*). (A) The full second derivative matrix. The self-second derivatives are situated along with main diagonal and visualized with a black border. (B) Isolated self-second derivatives. Purple means negative value, whereas green positive.

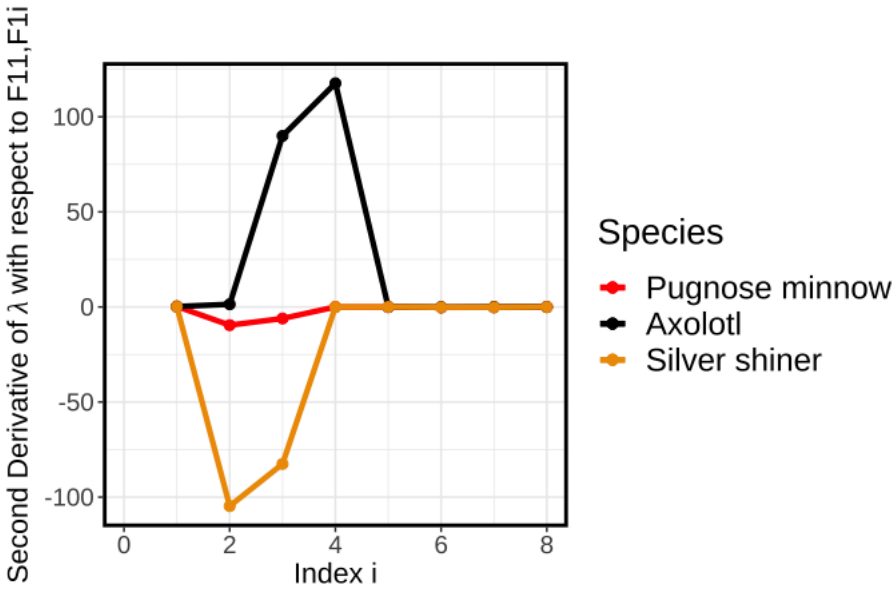

Figure A.5: Caption